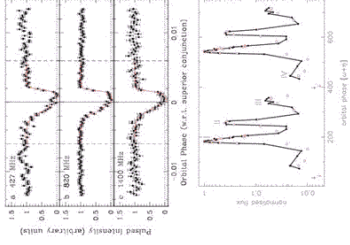
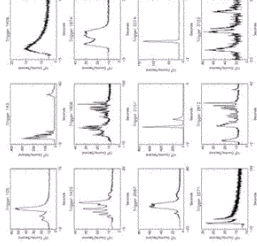
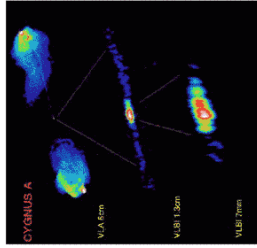
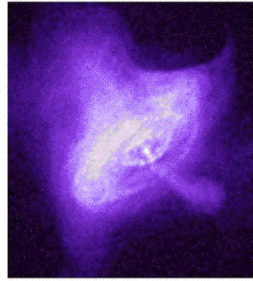


# Shock Waves and Flow Structure in Relativistic Winds and Jets

Jonathan Arons  
University of California, Berkeley



Pulsar Winds (Crab) Radio Sources (Cyg A)

Gamma Ray  
Bursts

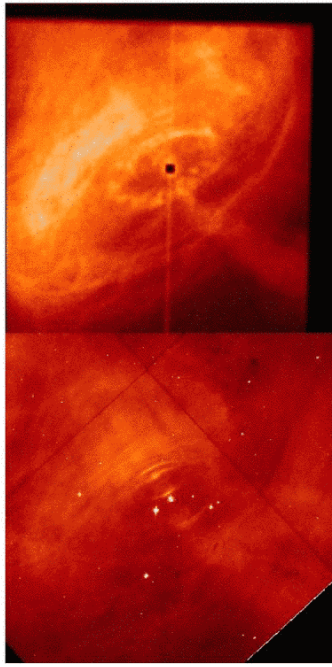
PSR J 0737 A&B

With a little help from my friends: **D. Alsop**, **E. Amato**, **D. Backer**, **B. Gaensler**, **Y. Gallant**,  
M. Hoshino, V. Kaspi, A.B. Langdon, C. Max, **A. Spitkovsky**, M. Tavani

1

## Astrophysical Motivation

Scale:  $10^{18}$  cm



Relativistic Motion

1) Winds from Rotation Powered Pulsars

Crab: Time  
Dependent  
Energy  
Deposition

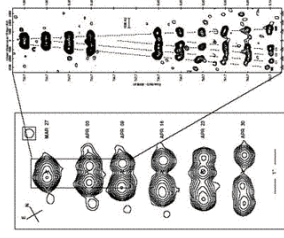
Chandra and  
HST observations

Quasi-Period (?):  
5-6 months

Speed of features:  $\sim 0.5 c$   
Inferred upstream  
4-speed  $10^{4-6}c$

2) Superluminal Expansion in Jets

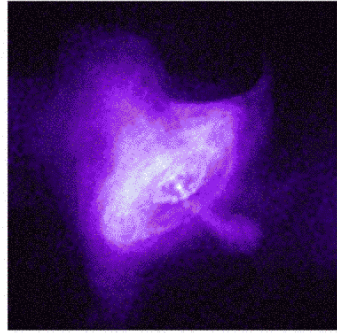
Galactic microquasar  
(Black hole in a binary)  
GRS 1915+105  
 $0.86c < v < 0.98c$



2

Observed Radiation: Incoherent Synchrotron from nonthermal, isotropic (?) particle populations (electrons, electrons + positrons)

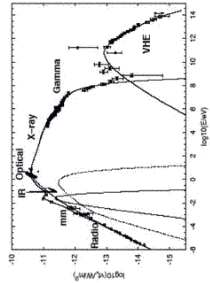
Pulsar Wind Nebulae



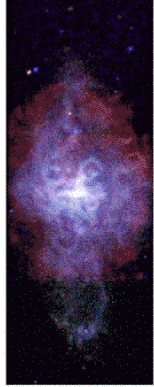
0.5 pc

Crab X-ray

$$\dot{E}_R = 5 \times 10^{38} \text{ erg / s}, \Gamma_{\text{wind}} \approx 10^6$$



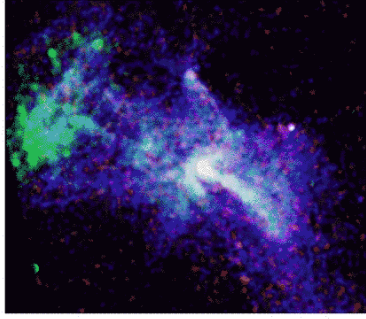
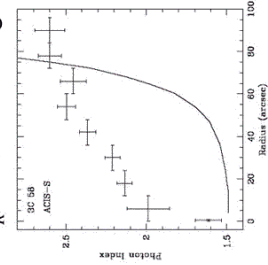
$$F_\epsilon \propto \epsilon^{-p} \text{ (photons/keV-s-cm}^2\text{)}$$



4 pc

3C58 X-ray

$$\dot{E}_R = 2.5 \times 10^{37} \text{ erg / s}$$

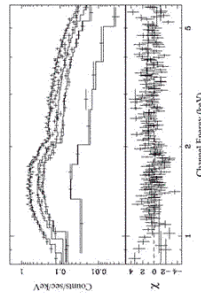


10 pc

G320/PSR1509-58

X-ray

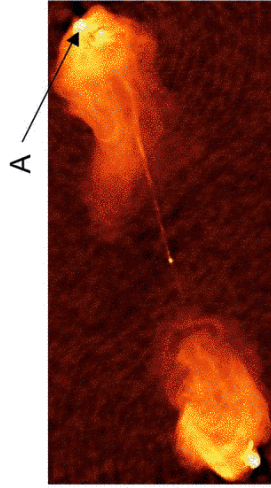
$$\dot{E}_R = 1.8 \times 10^{37} \text{ erg / s}$$



Central powerhouse - low emission transmission (MHD wind?) - large emission starts abruptly beyond well defined radius

$$p=2 \quad 3$$

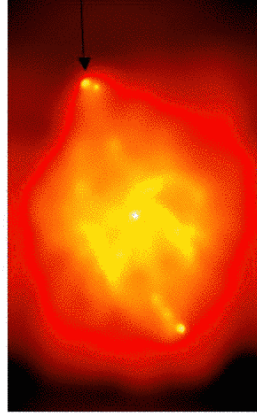
Radio Galaxies - Jets from Black Holes



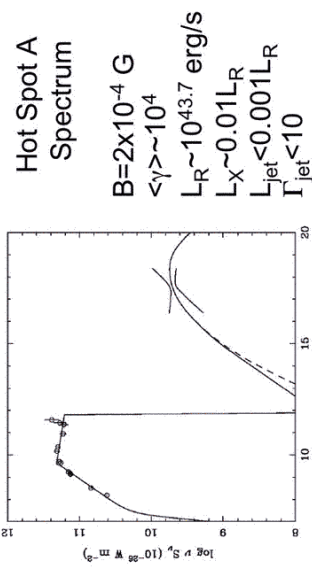
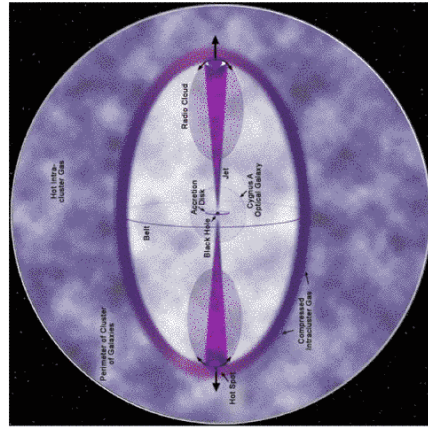
200 kpc

Cygnus A - Radio (6 cm)

Nonthermal Synchrotron Emission



Cygnus A - X-Ray (1-5 keV)  
Compton Upscatter of Radio Emission



Hot Spot A  
Spectrum  
 $B=2 \times 10^{-4} \text{ G}$   
 $\langle \gamma \rangle \sim 10^4$   
 $L_R \sim 10^{43.7} \text{ erg/s}$   
 $L_X \sim 0.01 L_R$   
 $L_{\text{jet}} < 0.001 L_R$   
 $\Gamma_{\text{jet}} < 10$

Schematic

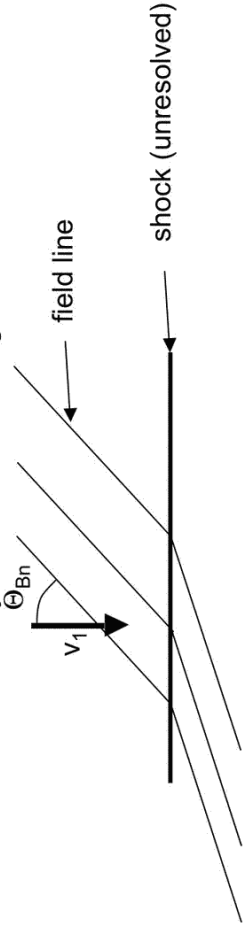
Central powerhouse - low emission transmission - large emission starts abruptly beyond well defined radius



Morphology: suggests sudden deceleration of magnetized relativistic flow - shock - as converter of flow energy to nonthermally heated electron (+ positron) spectrum  
 →  
 synchrotron emission in post-shock flow

Gamma Ray Bursts (Afterglows) - Relativistic jet ( $\Gamma \sim 10^2$ ) collides with ISM - spectrum of shocked ISM emits synchrotron (? could be non-linear inverse Compton = jitter) emission

“Shock acceleration” = efficient (>10% usually needed) conversion of flow energy to nonthermally heated broad (in energy) downstream particle population - usually assumed to be Diffusive first order Fermi Acceleration (DFA) - particles must access upstream from downstream many times while following B



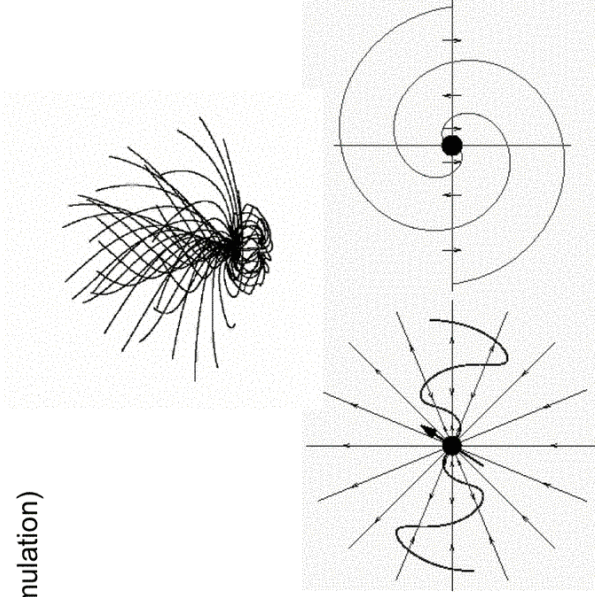
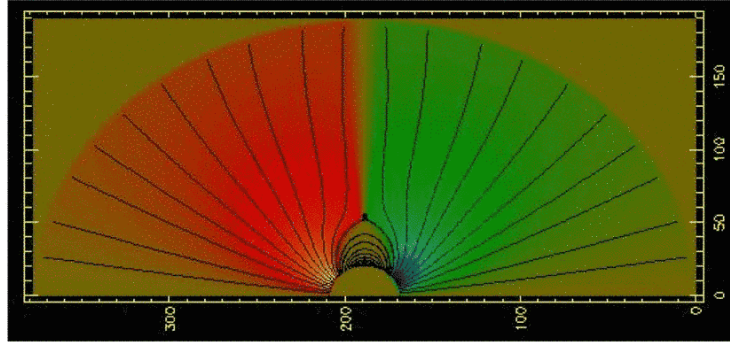
$v_1 \sim c$ : upstream access possible only when  $\tan \Theta_{Bn} < 1/\Gamma_1 \ll 1$   
 strong B transported from central source: B ~ perpendicular to flow  
 cross-field diffusion access from downstream requires very strong turbulence to scatter particles back upstream before advected away by fast flow ( $v_2 \sim c/3$  in shock frame) - what is post-shock turbulence?

Acceleration intrinsic to shock structure?

5

Upstream Flow - Relativistic Wind (Jet Issues Similar-hot spot params ~ PSR winds)

Wind from a Dipole (aligned - force free simulation)

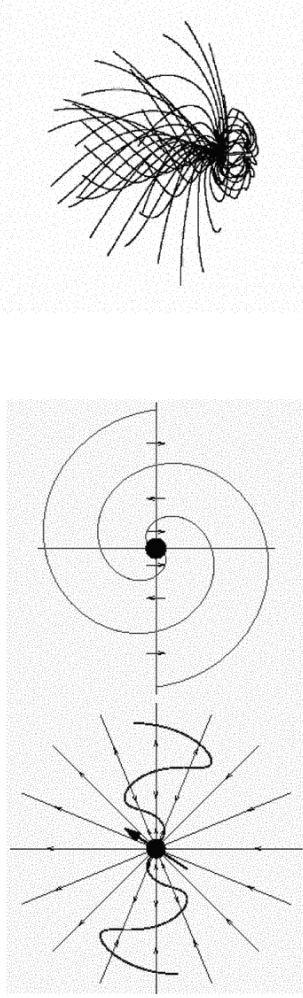


Asymptotic ( $r \gg R_L = c/\Omega$ ) Field Structure:  
 split monopole

Plasma content: electron-positron pairs + ions  
 in equatorial current sheet (current closure)

6

Oblique Split Monopole (Bogovalov 1999 MHD)



Field magnitudes and drifts ( $E \times B$ , polarization) same as aligned rotator

Toroidal field wraps with opposite sense in opposite hemispheres

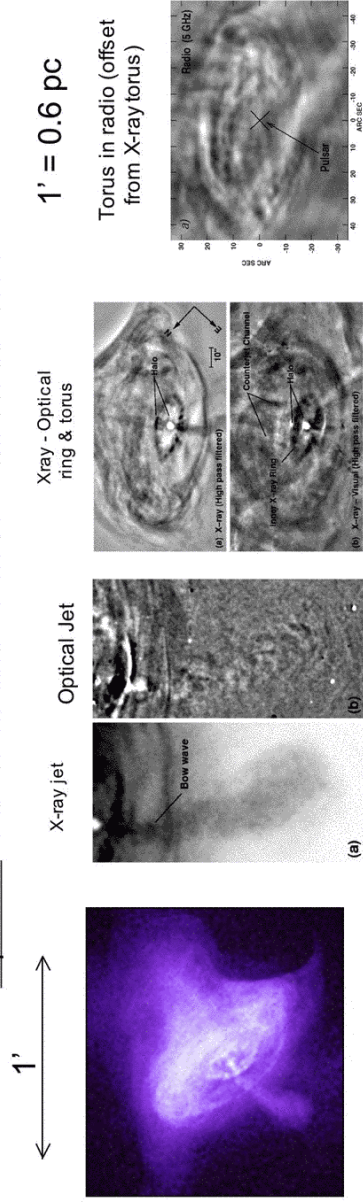
Field alternates sign between current sheet crossings in equatorial sector of opening angle  $2\iota$ ,  $\iota$  = angle between rotation axis and magnetic moment - crinkled current sheet = frozen in wave

$$\text{Wind characterized by ratio of Poynting flux to kinetic energy flux} \quad \sigma \equiv \frac{B^2}{4\pi m v c^2} \gg 1$$

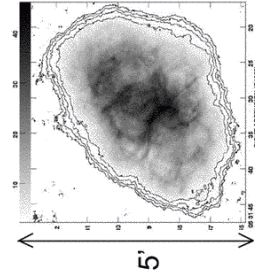
$$rB = \text{constant}, \quad r^2 n c = \text{constant} \\ \Rightarrow \sigma = \frac{\sigma_0}{\gamma}, \quad \sigma_0 \equiv \left( \frac{B^2}{4\pi m v c^2} \right)_{r=R_L} \approx 2 \times 10^6 \text{ (standard Crab } e^\pm)$$

$$\gamma = \text{constant} \Rightarrow \sigma \gg 1 \text{ everywhere} \quad 7$$

Equatorial Wind Termination - the Kennel and Coroniti View



Crab in X-Rays



Kennel and Coroniti (1984) spherical (sector) model

$$\sigma_1 \sim 5 \times 10^{-3}, \gamma_1 \sim 10^6,$$

$$\dot{N}_\pm (O - X - \gamma) \approx 3 \times 10^{38} \text{ s}^{-1} \sim 10^4 \dot{N}_{GJ} \Rightarrow \text{MHD}$$

$$[\dot{N}_{GJ} = \frac{2\Omega^2 \mu}{c q} = 2 \times 10^{34} \text{ s}^{-1} \text{ (Crab, ...)}]$$

Crab in Radio

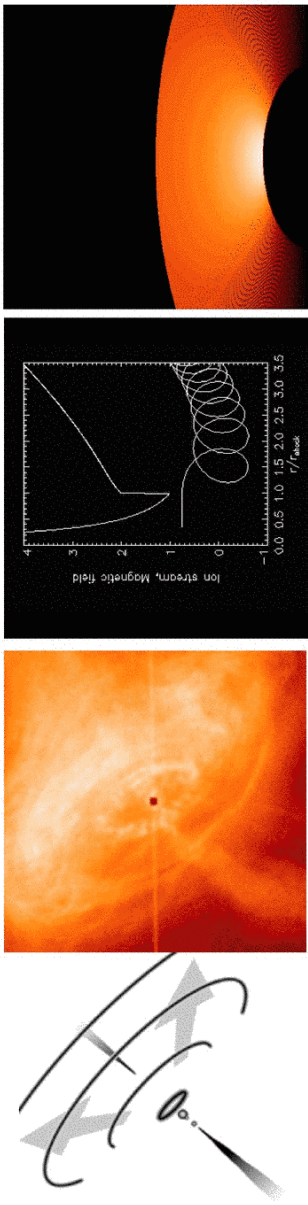
$$\langle \dot{N}_\pm (\text{radio}) \rangle \approx 10^{40} \text{ s}^{-1} \text{ (slow, dense, higher latitude flow?)}$$



Modeling of termination shock, nebular flows outside of shock yields  $\sigma(r=R_{\text{shock}}=10^9 R_L \ll 1) \sim 0.01$

### Ion Doped Equatorial Shock (Kinetic Ions/MHD pairs - 1D)

(Spitkovsky and Arons, Ap J 2004)



#### Parameters of ion doped shock model

Represents equatorial wind angular sector = crinkled current sheet sector

$\sigma_1 \sim 5 \times 10^{-3}$ ,  $\gamma_1 \sim 3 \times 10^6$ ,  $m_p c^2 \gamma_1 = 0.15 e \Phi_{\text{magnetosphere}}$ ,  $\gamma_1 = e \Phi_{\text{magnetosphere}} / m_{\text{eff}} c^2$   
 $\dot{N}_i \approx \dot{N}_{GJ} = 2 \times 10^{34} \text{ s}^{-1}$ ,  $\dot{N}_+ \approx 3 \times 10^{38} \text{ s}^{-1} \sim 10^4 \dot{N}_i \Rightarrow \text{MHD}$ ,  $m_{\text{eff}} = [(m_i n_i / Z) + n_- + n_+] / n_{GJ}$

Equatorial flow = Electric Return Current + pairs

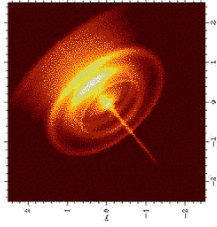
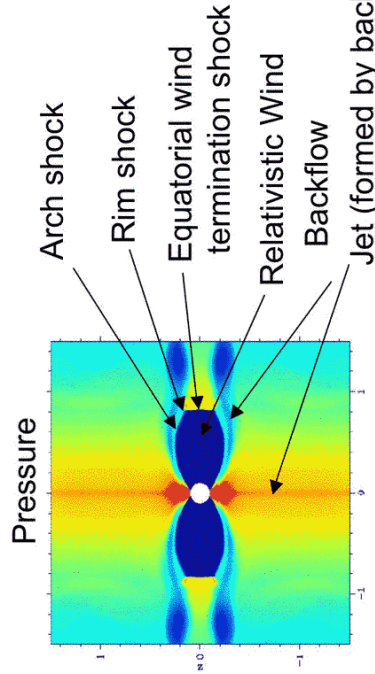
UHE ions yield UHE  $\gamma$  (HESS et al) & neutrinos (Ice Cube); HEGRA excludes  $\gamma_1 < 10^6$  wind

Pair injection rate comparable to polar cap and outer gap model predictions - does not address higher latitudes (higher density, lower 4 velocity?); "jets"?

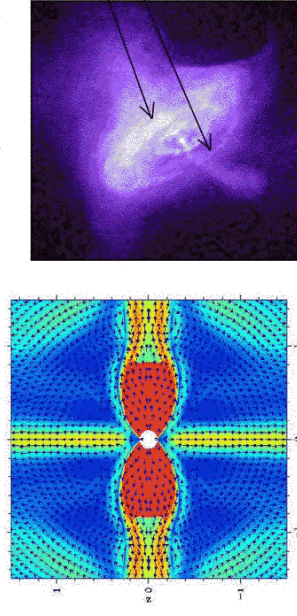
### Khangoulyan & Bogovalov 2002; Lyubarsky 2002; Komissarov & Lyubarsky (2003,2004); Del Zanna et al (2004) - 2D flow structure

2D electron-positron pairs/MHD models for nebular flow

Inject a wind in a broad cone,  
Poynting flux  $\sim (\lambda \sin \lambda)^2$ ,  $\gamma \gg 1$



Model requires  $1 \gg \sigma \approx 0.01$   
other parameters not constrained (any  $\gamma \gg 1$ );  
Kinetic & wave structure at shock neglected



Approaching side brighter than receding side;  $v \sim 0.5c$ : good for Doppler boost; How come no Doppler asymmetry for inner ring? Where did all polar Poynting flux go? How come no sign of shock termination? Polar wind carries high density, low  $\gamma$ ? Also high  $\sigma$ ?  
Energy "all" in equatorial outflow, plume is interesting but not of major dynamical significance

Existing Relativistic MHD wind theory (Michel 1969, Goldreich and Julian 1970, Beskin Kuznetsova & Rafikov 1998) yields

$$\gamma_\infty = \sigma_0^{-1/3}, \sigma_\infty = \sigma_0^{2/3} \gg 1$$

Magnetic pressure accelerates flow only when outflow speed less than magnetosonic speed:

$$v = c \left( 1 - \frac{1}{\gamma^2} \right)^{1/2} < v_A = \frac{c}{\sqrt{1 + \frac{4\pi\rho\gamma c^2}{B^2}}}$$

⇒

$$M_F^2 \equiv \frac{(\gamma\beta)^2}{u_A^2} = \frac{\gamma^3}{\sigma_0} < 1, u_A^2 \equiv \frac{B^2}{4\pi\rho\gamma c^2} = \text{Alfvén speed} = \frac{\sigma_0}{\gamma}$$

Flow outruns its driving magnetic spring when  $M_F > 1$ , not when  $\gamma > \sigma_0$

Force free ( $\gamma = r/R_L$ ) works for  $M_F < 1$ , therefore  $(r/R_L)^3 < \sigma_0$ , (Beskin et al 1998); wind coasts ( $\gamma \sim \text{constant}$ ) for  $r > R_F$  with

$\sigma \approx \sigma_0^{2/3} \gg 1$ : magnetic tension almost cancels magnetic pressure

11

Physics of  $M_F = 1$ : ( $R_F = \sigma_0^{1/3} R_L$  peculiar to monopole?)

$R_F/R_L$  smaller in more general poloidal fields? For example,

$A \propto r^{2+\nu}$  (straight poloidal field lines),  $\nu \ll 1$

$$\Rightarrow \frac{R_F}{R_A} \propto \frac{1}{\nu}$$

$R_F = \sigma_0^{1/3} R_A$  in field with weak  $B_\theta \neq 0$

But weak acceleration beyond  $R_F$  generally true in ideal MHD:

$$\text{Nonrelativistic flow: } M_F^2 = \frac{\frac{1}{2}\rho v^2}{\frac{B^2}{8\pi}} = \frac{\text{KE energy density}}{\text{EM energy density}} = \frac{v^2}{B^2 / 4\pi\rho} = \frac{v^2}{v_A^2} = M_F^2$$

$M_F < 1$ : EM dominated,  $v < v_A$ ;  $M_F > 1$ : KE dominated,  $v > v_A$

$$\text{Relativistic: } M_F^2 \equiv \frac{\gamma^3}{\sigma_0} = \frac{4\pi\rho\gamma c^2}{B^2} \gamma^2 = \frac{u^2}{u_A^2} = \frac{\text{KE energy density}}{\text{EM energy density}} \times \gamma^2 \leftarrow ?$$

12

EM Acceleration parallel to velocity: inertia anisotropic,  $m_{\text{eff}} = \gamma^3 m$

$$\rho c \beta \frac{\partial}{\partial r} (\gamma c \beta) = \rho c^2 \left( \beta \frac{\partial \gamma}{\partial r} + \gamma \frac{\partial \beta}{\partial r} \right) = \rho c^2 \gamma^3 \frac{\partial \beta}{\partial r} \sim - \frac{\partial B^2}{\partial r} \frac{B^2}{4\pi r}$$

EM velocity acceleration > Inertia:

$$1 > \frac{\rho c^2 \gamma^3 (\partial \beta / \partial r)}{B^2 / 4\pi r} = \gamma^2 \frac{4\pi \rho c^2 \gamma}{B^2} r \frac{\partial \beta}{\partial r} \approx M_F^2 \Rightarrow$$

Relativistic MHD winds (jets also?) accelerate to

$$M_F \approx 1 \left( \text{not } \sigma = \frac{\sigma_0}{\gamma} = 1 \right), \Rightarrow \gamma_\infty \approx \sigma_0^{1/3}$$

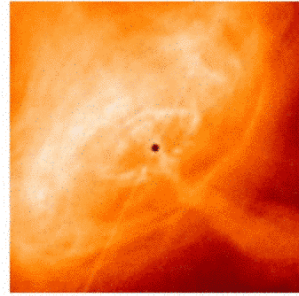
(not  $\gamma_\infty \approx \sigma_0$ )

Observations require stronger, non-radiative (equatorial) acceleration for  $r \gg R_F \sim (10^2 - 10^3) R_L$

13

Equatorial (Electro)Magnetic Dissipation? (Non-ideal flow)

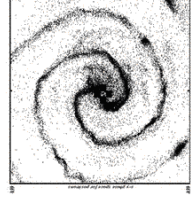
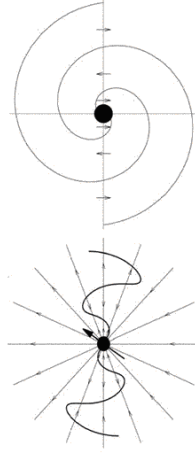
$$\Rightarrow \sigma(R_F) \sim \sigma_L^{2/3} \gg 1 \rightarrow \sigma(R_{shock}) \ll 1$$



Equatorial outflow

Return current "sheet" (current closes in Nebula - ion doped shock model has ~ full current to Nebulae in equator)

Oblique rotator's sheet = frozen in wave: dissipative?



Spitkovsky PIC simulation (unpublished)

Bogovalov's (1999) monopole solution

14

I. Current Sheet = sheet pinch (pressure inside sheet = magnetic pressure between sheets - Michel 1971, 1994, Coroniti 1990, Kirk et al,...)

“Reconnection” dissipates sheets and all B field between sheets in equator - “resistivity” = ? observational signature? How complete can the dissipation be? (Kirk & Skaeraasen 2003)

II. Current Sheet = sheet unstable to shear generation of strong EM waves (slipping stream, kinks)

III. MHD (Kink?) instability of the toroidal field in the wind? (breaks acceleration parallel to v)

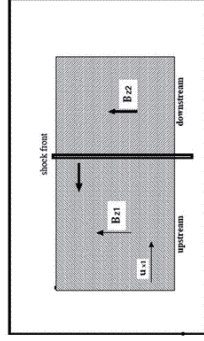
Observations needed: find a PWN with observer's LOS close to rotational equator - look head on into wind, see beamed radiation from dissipation layer

Anything useful from blazar, GRB?

15

Microscopic Shock Structure - PIC - do relativistic shocks thermalize? Do they “thermalize” to a non-thermal distribution? Do they have DFA? Are they significant coherent radio emitters

- I. 1D simulations with Upstream magnetic field structured only on flow scale (or absent)
  - a. Pure electron-positron
    - i. Transverse geometry - B perpendicular to the flow (Gallant et al 1992; Hoshino 2002; Amato and Arons, in prep; also Smolsky and Usov 1996 (barrier reflection))



Left wall: cold neutral  $e^\pm$ , speed  $c\beta_1 \mathbf{e}_x$ ,  $E_y/B_z = \beta_1$   
 Right wall: perfect conductor, specular reflection of  $e^\pm$

Simulation shown:  $\sigma_1=1$ ,  $\gamma_1=40$ , 1024 cells, 32 particles/cell,  $r_{L1}=10\Delta x$ ,  $\Delta t=0.9\Delta x/c$

Simulation Geometry

Results same for 512 and 2048 cells,  $r_{L1}=5\Delta x$ , particles/cell = 8, 16, 32, 64

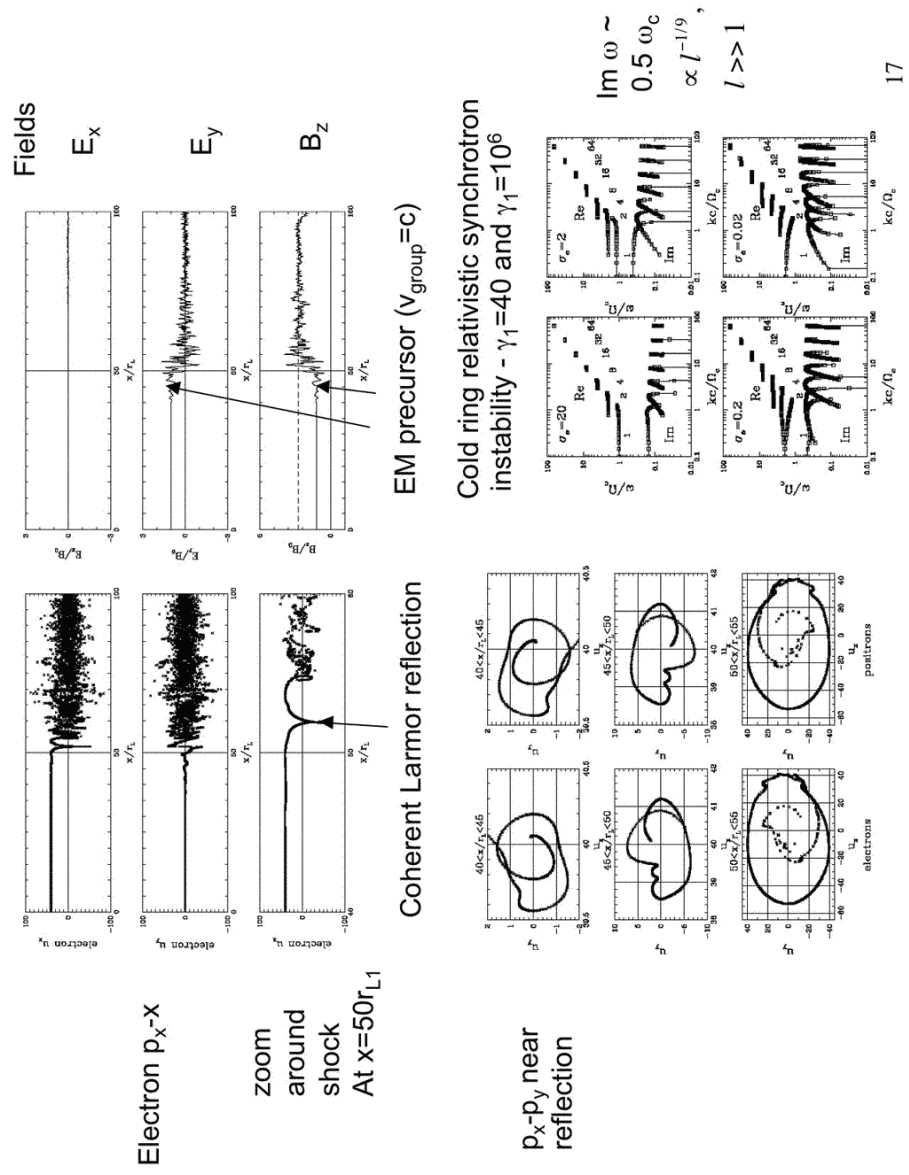
t=0: uniform moving plasma and fields fill box

Results very similar (in 1D) for  $\sigma_1=0.005, 0.01, 0.1$

After initial bounce off the wall (bounce similar to barrier reflection) well defined shock forms, travels upstream - downstream plasma at rest in simulation frame

16





17

**Thermalization (downstream)**

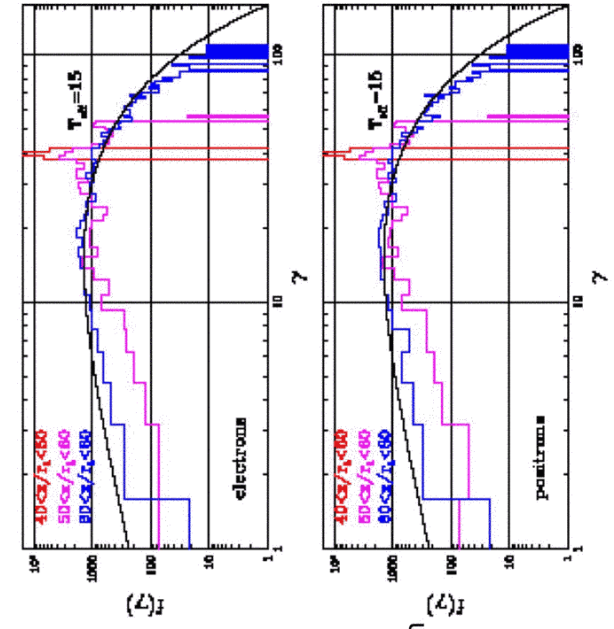
Rapid emission and absorption of synchrotron waves for

$$\omega \geq \omega_{UH} = \sqrt{\omega_p^2 + \omega_c^2} = \omega_c \sqrt{\frac{1 + \sigma}{\sigma}}$$

creates a local hohlraum, plasma thermalizes in  $10-20r_L$  ( $10-20 c/\omega_p$  when  $\sigma \ll 1$ )

Downstream upper hybrid turbulence level small (LTE) - 1D kills cross field scattering anyway, can't see diffusion in DFA, if any

**EM Precursor (upstream)**



From Amato & Arons, in preparation

18

EM Precursor (upstream)

$\sigma_1=0.3$

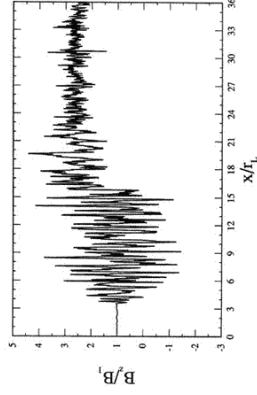
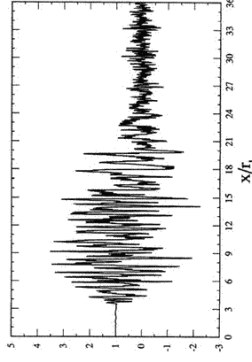
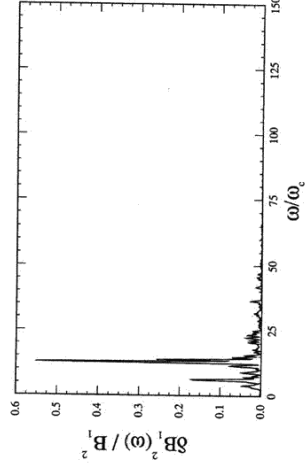


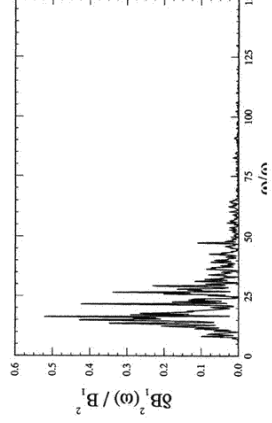
Fig. 1a



Spectral peaks at  $\omega = n\omega_{c1}$ ,  $\omega > \omega_{UH}$   
 Luminosity  $\sim 4\%$  of shock energy  
 flux (shock frame)



$\sigma_1=0.03$



Possibly of relevance to high  $T_b$  in AGN day to day variable cm wave emission  
 (Gallant et al. 1992) - shocks in disk coronae

$$v \approx 3 \frac{B}{1 \text{ KG}} \left( \frac{0.01}{\sigma_1} \right)^{1/2} \frac{10}{\gamma} \text{ GHz}, \quad T_b \approx 10^{24} \frac{f_{\text{L}}}{0.01 \sqrt{0.1}} \left( \frac{\gamma_1}{10} \right)^3 \left( \frac{10^3 \text{ G}}{B_1} \right) \text{ K}$$

II. 3D simulations with upstream magnetic field structured only on flow scale (or absent)  
 (Spitkovsky and Arons, in preparation)  
 Motivation - PSR J7037A&B

Pulsar A

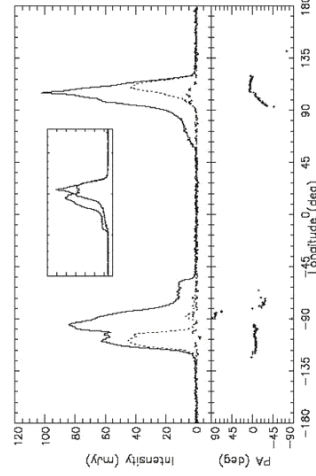
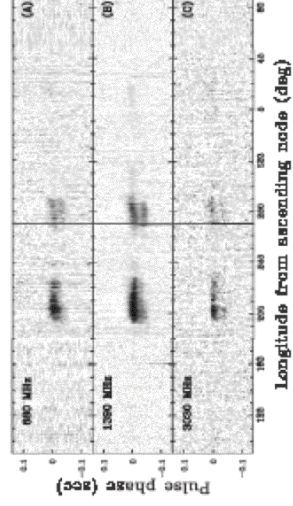


FIG. 1. — Polarization characteristics of J0737-3039A at 0.82 GHz. The inset gives the two portions of the profile ‘narrow-folded’ to show similarity of outer edges. See text for details.

- $P_A = 22.7 \text{ msec}, \dot{E}_A = 6 \times 10^{33} \text{ ergs / s}$
- $P_B = 2.77 \text{ sec}, \dot{E}_B = 2 \times 10^{30} \text{ ergs / s}$
- $R_{LA} = 1098 \text{ km}, R_{LB} = 132,400 \text{ km}$
- $B_A = 6.3 \times 10^9 \text{ G}, B_B = 0.4 \times 10^{12} \text{ G}$
- $2a = 850,000 \text{ km}$

Lyne et al (2004)

Pulsar B



Pulsar B brightness as a function of rotation phase (vertical axis) and orbital phase (horizontal axis) - Lyne et al (2004 - discovery paper)

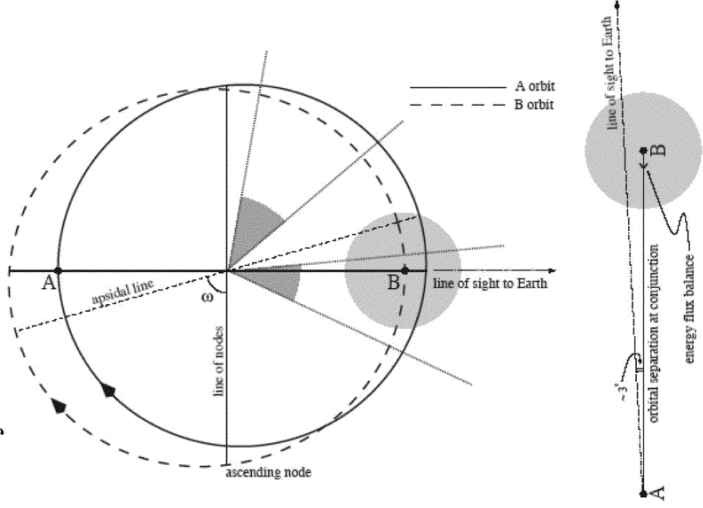
Ramachandran et al 2004

Doppler shifts of pulse periods allow  
 measurement of orbital parameters

Lyne et al (2004)

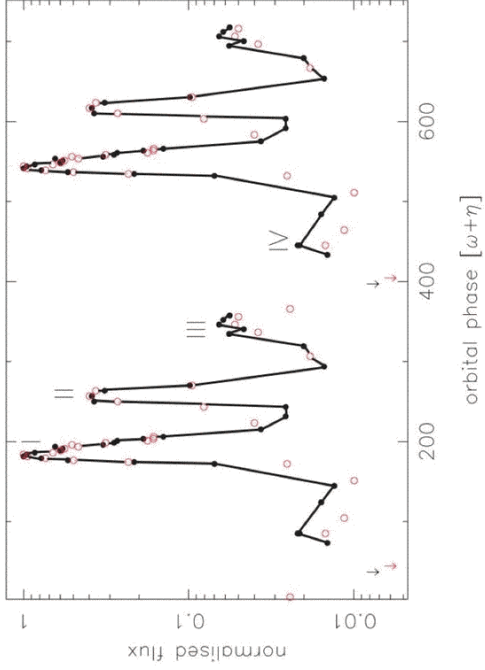
PSR J0737 A&B -- laboratory for relativistic winds

Binary orbit:



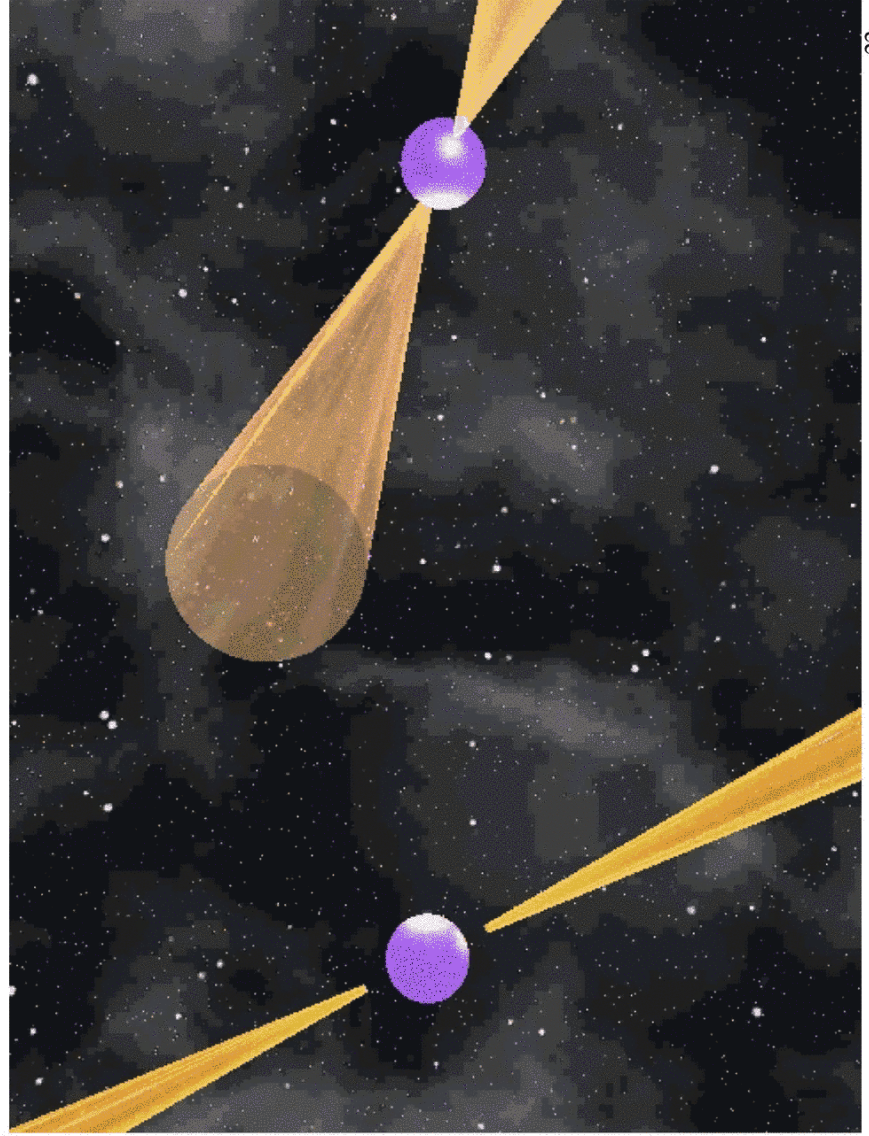
Eccentricity: 0.0878  
 Characteristic age: 270 Myr(A), 50Myr(B)  
 Mass ( $M_e$ ): 1.33 1.25  
 Orbital inclination: 90.3 (Ransom 04)

Pulsar B Light Curve



Ramachandran et al (2004) 21

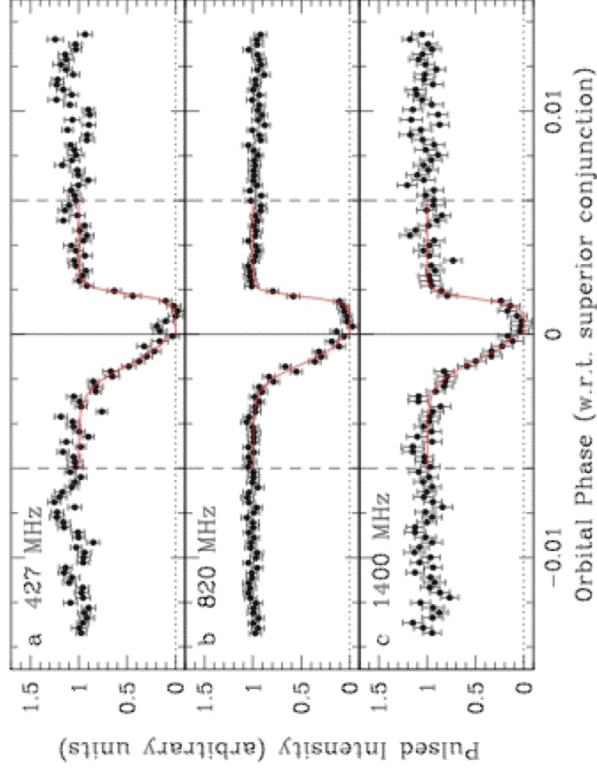
Lyne et al (2004)



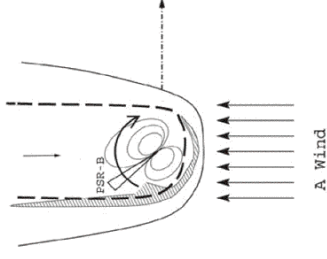


## Eclipses of Pulsar A

Lyne et al 04, Kaspi et al 04 see brief eclipse of A when pulsar B moves in front of A



Pulsed flux of pulsar A for 4 minutes centered on superior conjunction (A behind B). Each data point is a 2 s integration. The eclipse lasts ~30 s, corresponding to a 18,600 km physical dimension of the obscuring material along the direction of orbital motion.



Cartoon of eclipse model - magnetosheath absorption by PSR B 23

Eclipse is asymmetric and shortens at higher frequencies (Kaspi et al 04)

## PIC (!) simulation of wind-magnetosphere interaction

### Simulation setup:

Relativistic  $e^\pm$  wind ( $\gamma = 10-50$ ) with toroidal B field ( $\sigma = 0.1-3$ )  
 Inflate bubble of rotating inclined dipole magnetic field  
 No plasma initially in the magnetosphere, no surface emission

### We use particle-based simulation (PIC)

Advantages: fully kinetic, self-consistent collisionless shocks, reconnection physics included automatically  
 Disadvantages: plasma scales have to be resolved;

magnetosphere = 50 skin depths; huge simulations

This is doable for pair plasma (no ion scales) - relevant when

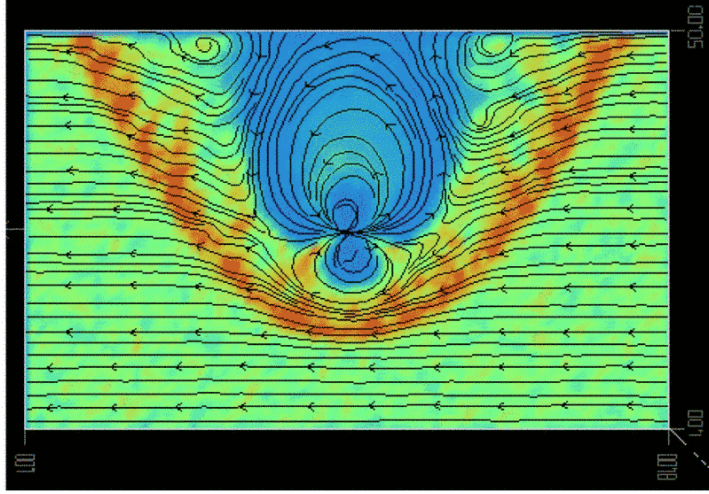
B is not in rotational equator plane of A (90% of orbit)

Relativistic MHD behavior is reproduced.

### Code "TRISTAN":

- 3D cartesian electromagnetic particle-in-cell code
- Algorithms for rotating magnet
- Handles magnetized flows
- Fully parallelized (128proc+) - parallelized in tubes along flow
- Resolution requirements: typical run  $512^3$  grid,  $6 \times 10^8$  particles, 50+ Gb. 24

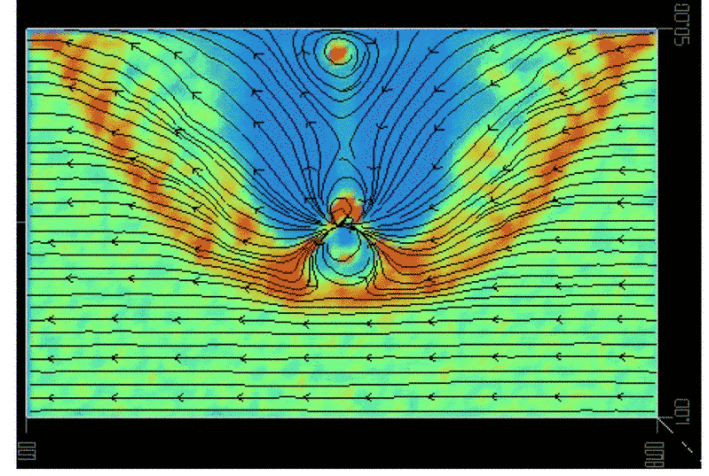
Shock and magnetosheath of pulsar B



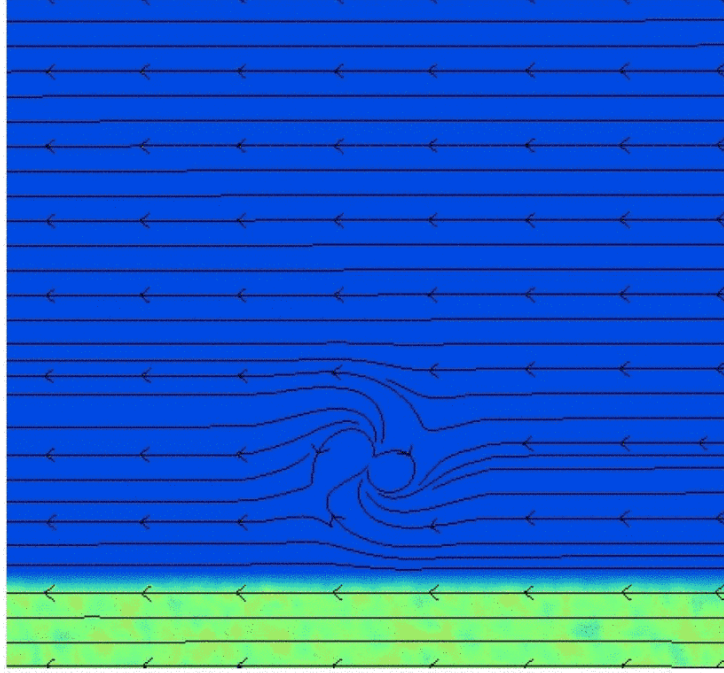
No "dayside" reconnection

*Similar to the interaction between Earth magnetosphere and solar wind.*

*With "dayside" reconnection  $\eta_{25}$*



Shock and magnetosheath of pulsar B: effects of rotation



*Shock modulated at  $2\Omega$*

*Reconnection once per period*

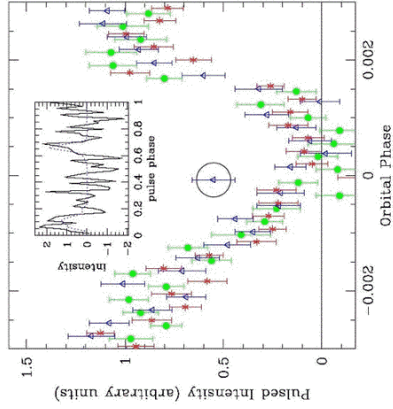
*Cusp filling on downwind side*

*Density asymmetries*

*$R_m \sim 50000$  km*



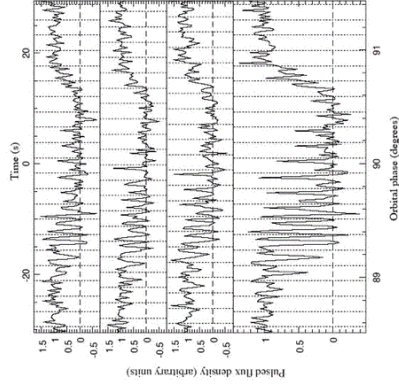
Detailed A eclipse light curves (Kaspi et al 2004, McLaughlin et al 2004)



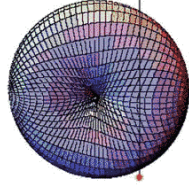
1400 Mhz, low time resolution

High resolution shows doubly periodic modulation early in eclipse, changes to singly periodic late in eclipse

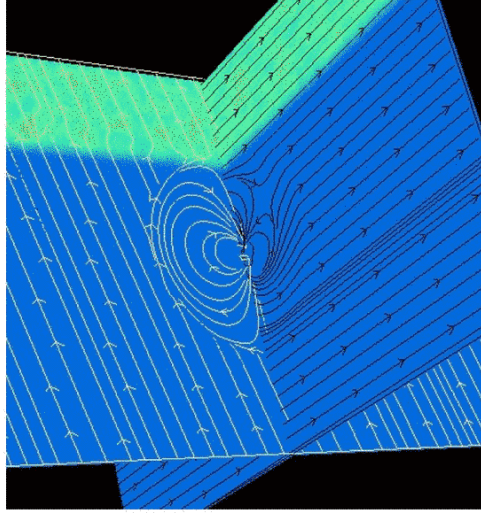
Suggests absorption by plasma **inside** B's magnetosphere (Rafikov and Goldreich 2004, Lyutikov & Thompson 2005) - plasma trapped on dipole field lines (like van Allen belts of Earth)



800 Mhz, high time resolution



### 3D magnetosphere

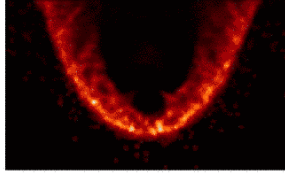


Optical depth: dark= low  $\tau$

### A Eclipse and synchrotron absorption

To explain weak frequency dependence of eclipse, need to have high optical depth. Used synchrotron absorption in isotropic thermal plasma as the eclipse mechanism:

$$\tau_\nu = \frac{\sqrt{3}cr\theta_{\perp}R_m}{v_g T_e B_z} \left( \frac{v_{cl}}{v} \right)^2 I(z) = \frac{2}{v_{pl00}^2} \left( \frac{\kappa}{10^6} \right)^2 f(\sigma), \kappa = \frac{\theta_{\perp}}{r_{cl}}$$



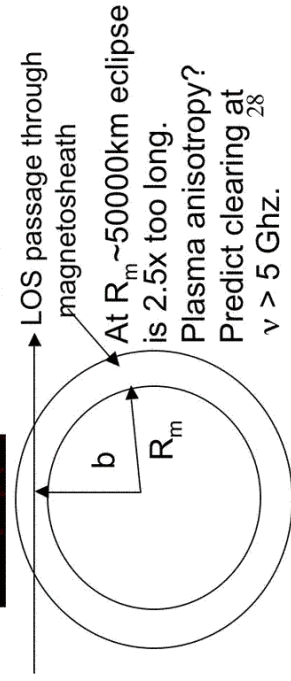
eclipse requires:

$$\kappa \sim 3 \times 10^6, \gamma_1 \sim 10,$$

$$\sigma_1 \sim 1$$

The wind is too dense and too slow according to conventional wisdom.

Plasma gyrophase coherence?



At  $R_m \sim 50000\text{km}$  eclipse is 2.5x too long. Plasma anisotropy? Predict clearing at  $\nu > 5 \text{ GHz}$ .



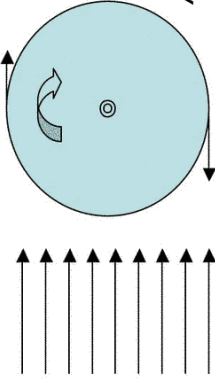
Spindown of pulsar B -- wind torques

How does PSR-B spin down?

1) "Regular" spindown through the tail of the magnetosheath.

$$(\dot{J}_B)_{spindown} = \frac{\dot{J}_B}{\Omega} = \frac{\mu^2 \Omega^3}{c^3} \left( \frac{R_m}{R_{LB}} \right)^2 \sim 10^{29} \text{ ergs}$$

2) "Propellor" torque.



In case of PSR-B coupling to the flow is provided through reconnected field.

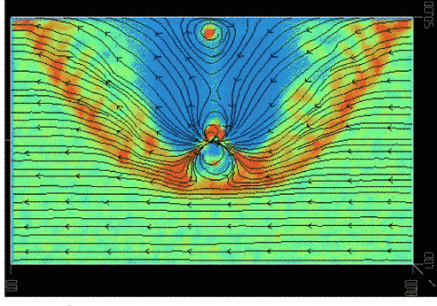
Acceleration on the dusk side, deceleration on the dawn side.

$$(\dot{J}_B)_{propellor} \propto \rho v \Omega R^4$$

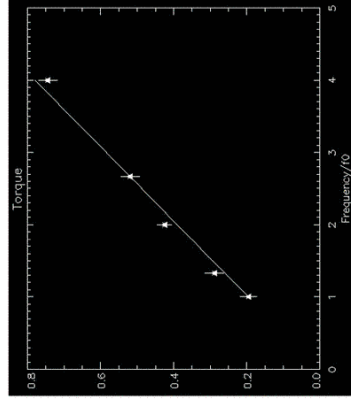
$$(\dot{J}_B)_{rec} = \int dV \left( \mathbf{r} \times \frac{1}{c} \mathbf{j} \times \mathbf{B} \right) \cdot \hat{\Omega}_B \sim \left( \frac{\dot{J}_A}{a^2 c} \right)^{1/3} \mu^{4/3} \frac{\Omega_B}{2c\beta_{||}} = 2 \times 10^{30} \text{ ergs}$$

The wind torque is larger than the regular spindown torque!

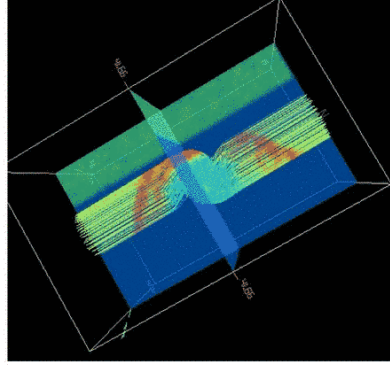
This leads to more accurate B field:  $4 \times 10^{11} \text{ G}$ .  $R_m = 50000 \text{ km} = 38\% R_{LB}$  <sup>29</sup>



Simulations show linear scaling of torque with  $\Omega_B$

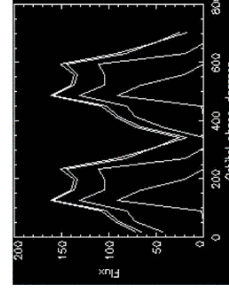
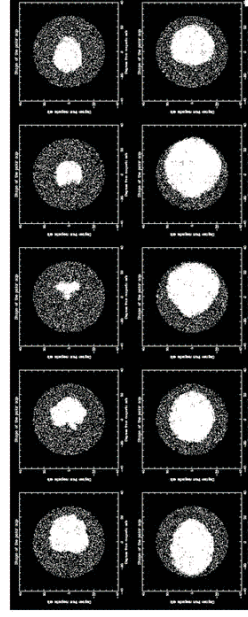


3D magnetosphere: fieldlines



Emission morphology of pulsar B

Polar cap size for different phases of the orbit (lines connected to the wind), at fixed rotation phase of B (magnetic pole pointing to observer):



Many Questions imply 3D shock structure simulations in  $e^\pm$  needed

Collective synchrotron absorption (& emission - unpulsed emission from binary is collective): density lower,  $\gamma_1$  higher

Plasma in absorbing layer anisotropic - eclipse shorter

3D allows cross field diffusion - nonthermal heating in pure  $e^\pm$  ?

Spitkovsky and Arons, in progress

Simulation setup: finite in x (400 cells), periodic in y (150), z (150): 9M cells particles bounce off x = 400 wall; radiation boundary conditions (Lindman) at x=0, x=400

$\sigma_1 = 0.1 - c/\omega_p = 15$  (also 0, 0.003, 0.01; 1; 3)

$(\Theta_{BN})_{downstream} = 90^\circ, 75^\circ, 45^\circ, 15^\circ, 0^\circ$  (L=800 cells for parallel shock)

$\gamma_1 = 15$  for all calculations; 1;8;16 particles/cell - little difference seen - 3D forgiving

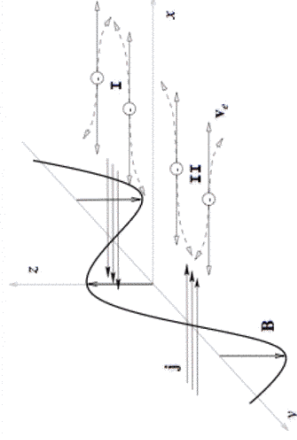
$(\tan \Theta_{BN})_{upstream} = \frac{1}{\gamma_1} (\tan \Theta_{BN})_{downstream} \Rightarrow$  Shock as if  $\sigma_1 = 0$  for  $(\Theta_{BN})_{downstream} < 45^\circ$  (?)

31

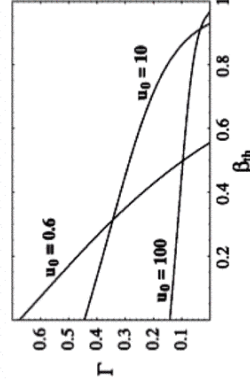
## Unmagnetized Pair shocks

*Why does a shock exist?*

Particles are slowed down either by instability (two-stream-like) or by magnetic reflection. Electrostatic reflection is important for nonrelativistic shocks and when ions are present.



*Weibel instability*



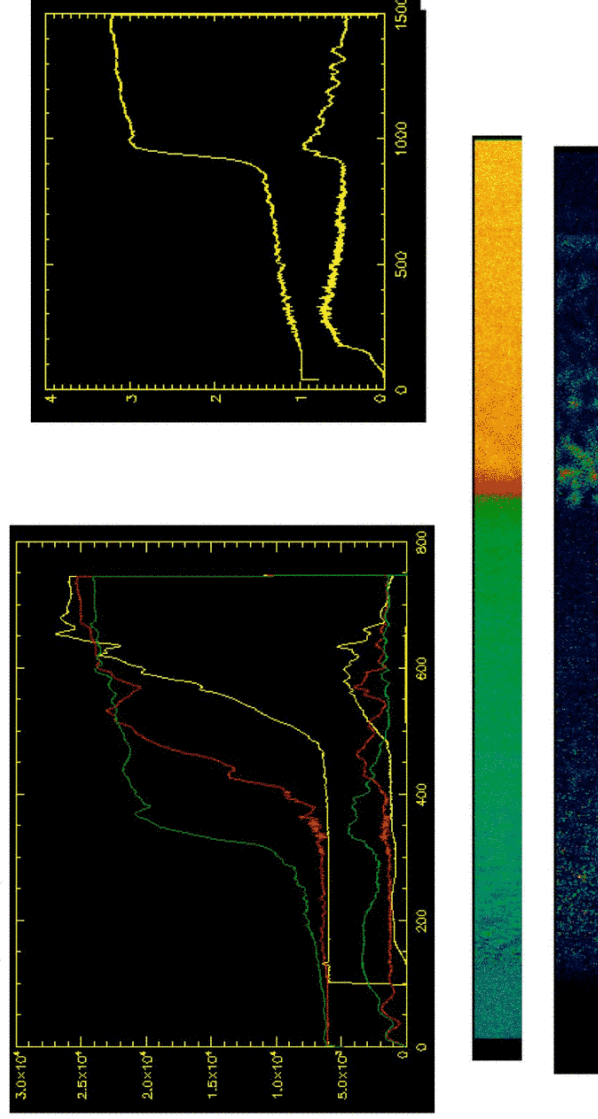
32

*Shock structure: Density evolution*

Shock transition is accomplished in roughly 20-50  $c/\omega_p$

**Shock structure: precursor**

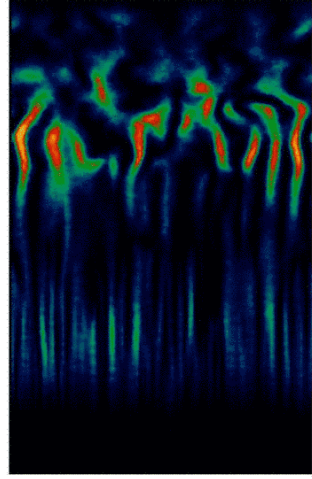
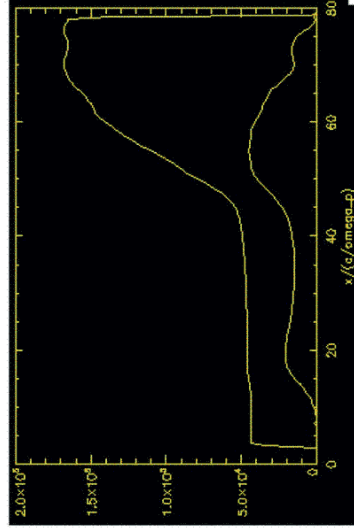
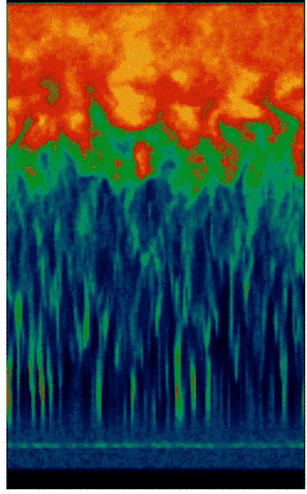
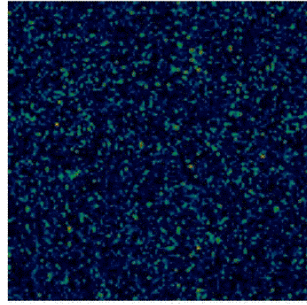
Streaming particles from the initial shell plow through the upstream medium, creating upstream turbulence. This modifies shock jump conditions. These particles (left over from the initial conditions) always outrun the shock.





### 3D shock structure

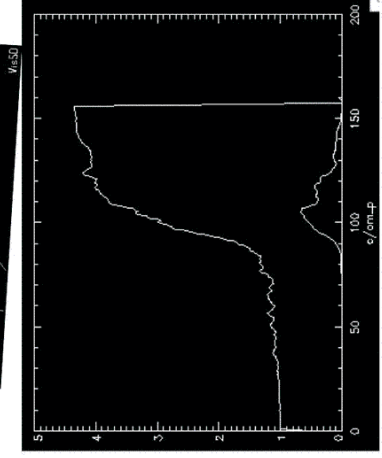
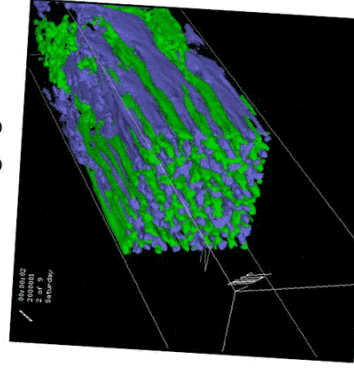
Evolution of field energy through the 3D shock structure, including the precursor.



35

### Magnetic field generation

Field cascades from  $c/\omega_p$  scale to larger scale due to current filament merging



36

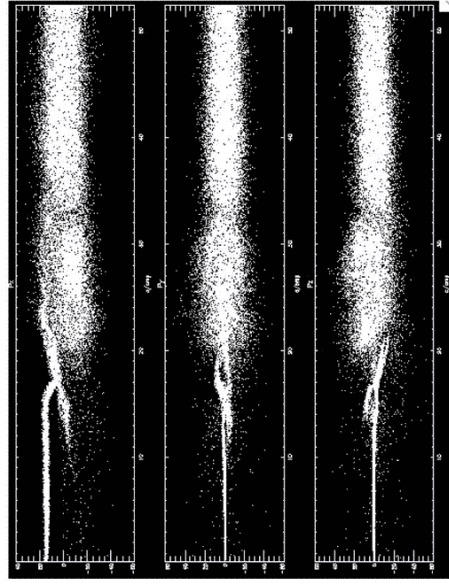
Weibel instability generates subequipartition B fields that decay. Asymptotic value declines toward zero - diffusion and inverse cascade.

$$\left( \frac{\delta B^2}{8\pi nT} \right)_{\sigma=0} \approx \left( \frac{\delta B^2}{8\pi \rho_1 c^2} \right)_{\sigma=0} \approx 0.01 \text{ (magnetic trapping)}$$

**Unmagnetized pair shock**

Particle acceleration

Particle spectrum

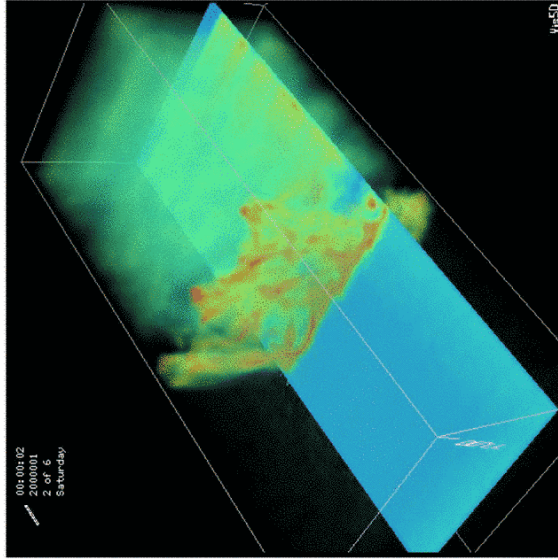


“No” nonthermal tail is created, particles are efficiently thermalized by interacting with the Weibel magnetic field. Thermalization leads to particles with energies up to  $4kT$  - turbulence too weak for DFA. Weak turbulence does scatter a very small fraction of particles.  
 Particle # - nonthermal tail efficiency  $< \exp(-4\gamma mc^2/T)$

**Magnetized perpendicular pair shock**

Shock structure  $\sigma=0.1$

Plane of  $v_x$ - $B_y$

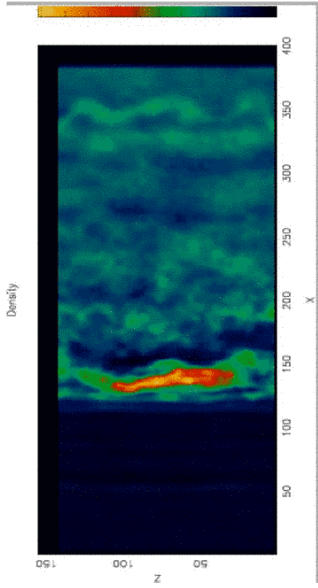


Plane of  $v_x$ - $E_z$

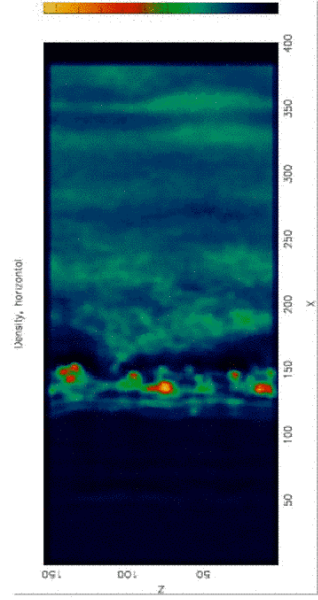
Shock is clearly magnetized -- anisotropy with respect to  $B$ . Shock thickness -- several Larmor radii.

$$\sigma_1 = 0.1, (\Theta_{BN})_{\text{downstream}} = 90^\circ$$

Density:  $E_0 - \langle v_x \rangle$  plane

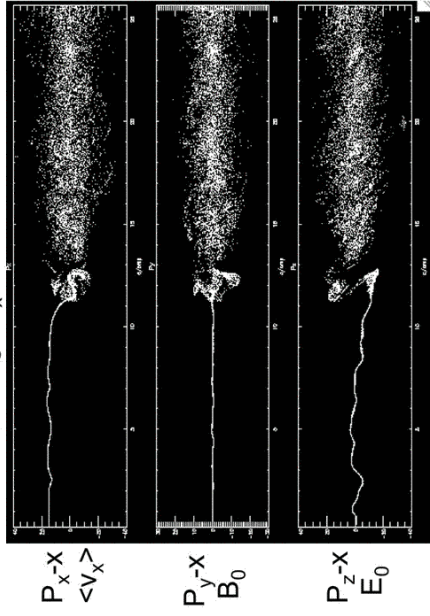


Density:  $B_0 - \langle v_x \rangle$  plane

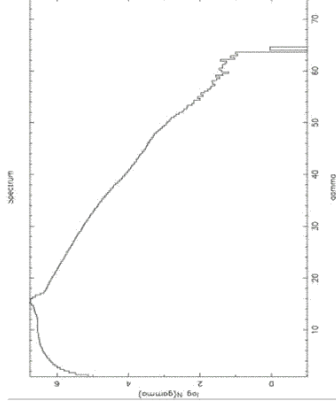


39

3D Phase space - a cut in middle of the box, along  $\langle v_x \rangle$  direction

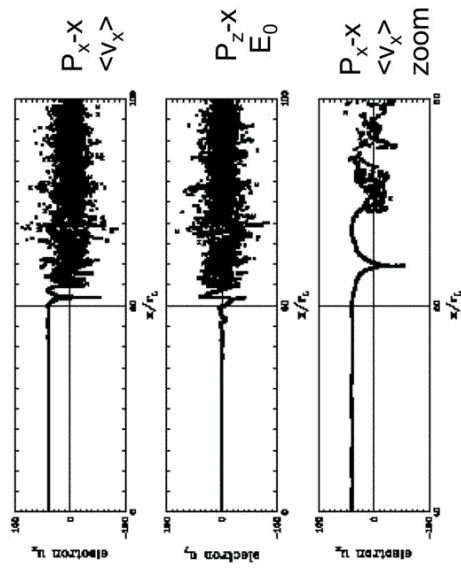


Intense gyrophase bunching in reflection region - maser

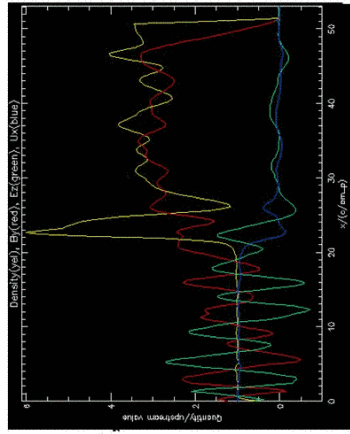


Downstream Spectrum: thermal

1D



Strong precursor as in 1D

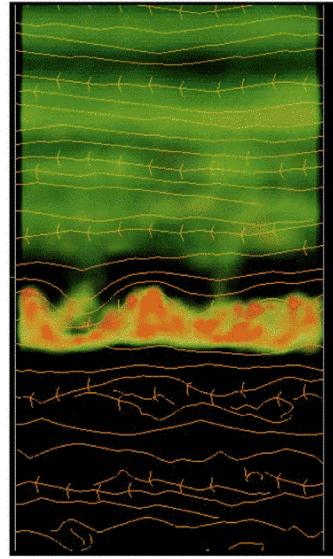
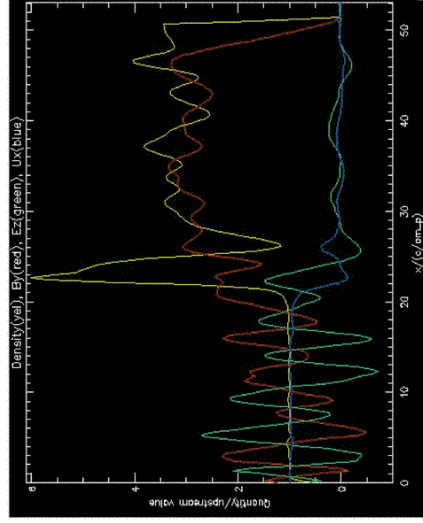


Magnetic reflection, cyclotron instability



### Magnetized perpendicular pair shock

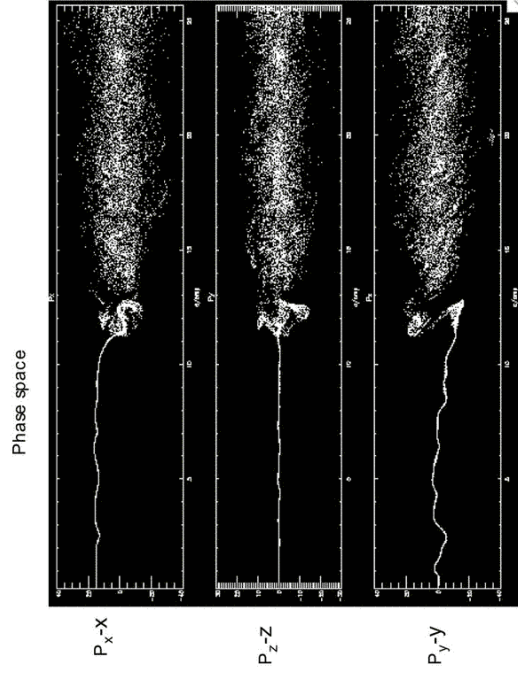
Shock structure  $\sigma=0.1$  -- electromagnetic precursor



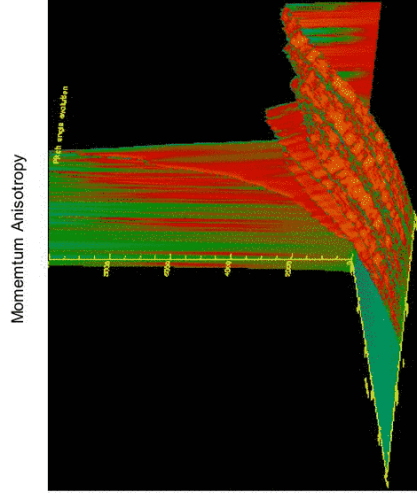
Shock compression is  $\sim 3$ .  
Plasma is quasi-2D with  $G=3/2$

41

### Magnetized perpendicular pair shock

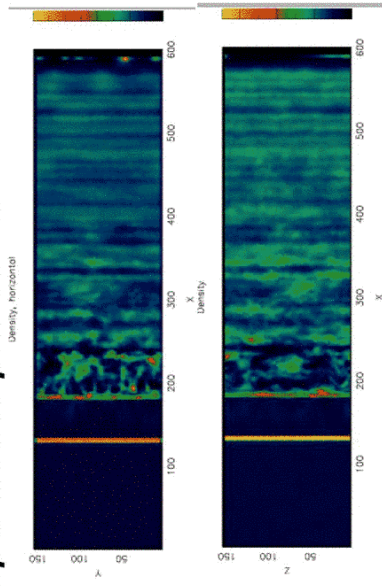
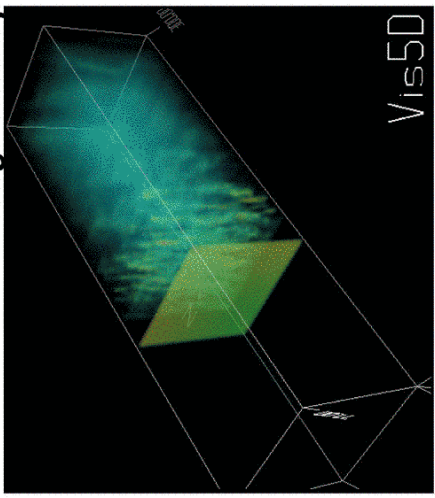


Shock structure dominated by magnetic reflections, as in 1D.  
No nonthermal acceleration even in 3D.

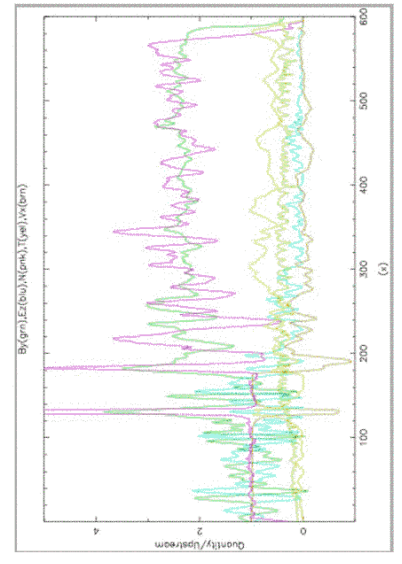
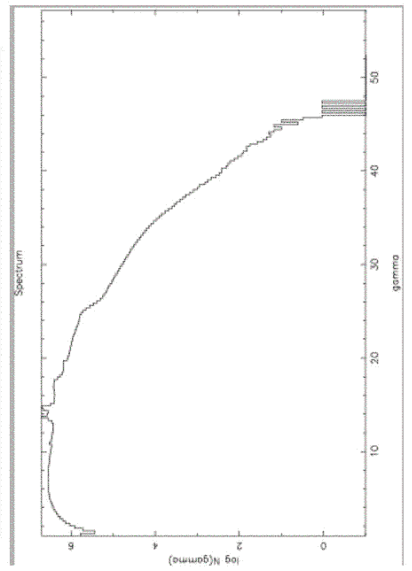


42

**Magnetized perpendicular pair shock**

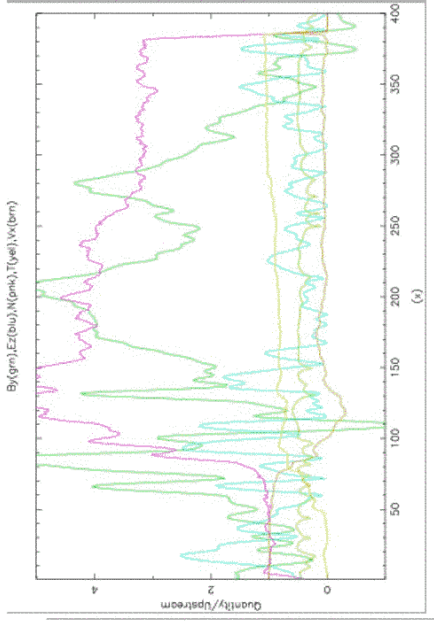
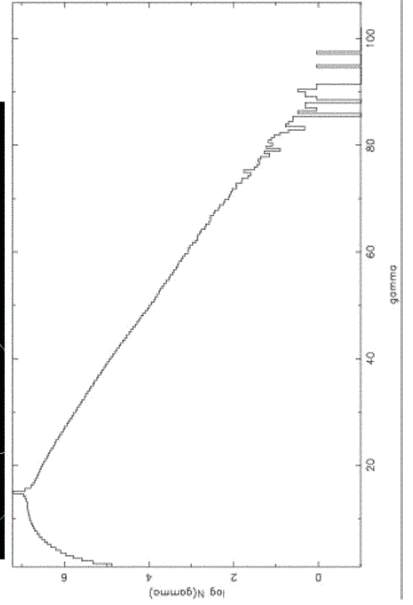
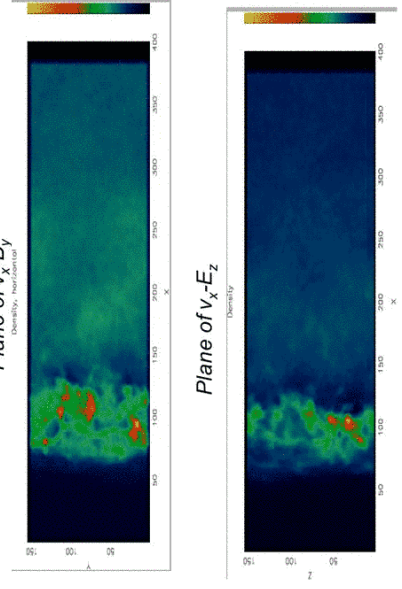
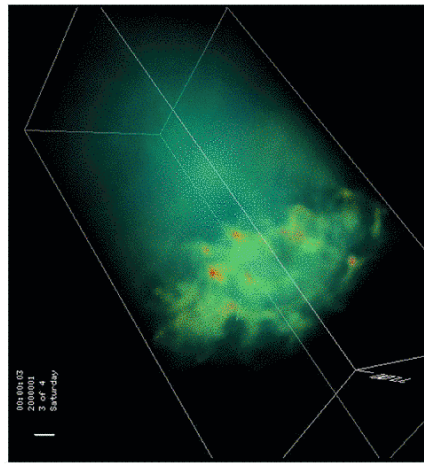


Gyrophase bunching persists



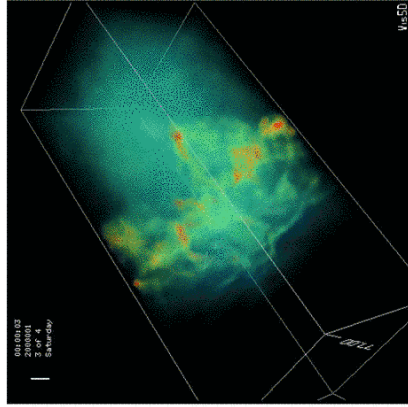
**Magnetized perpendicular pair shock**

Shock structure  $\sigma=0.01$

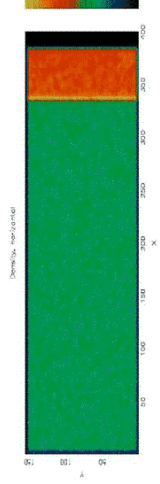


### Magnetized perpendicular pair shock

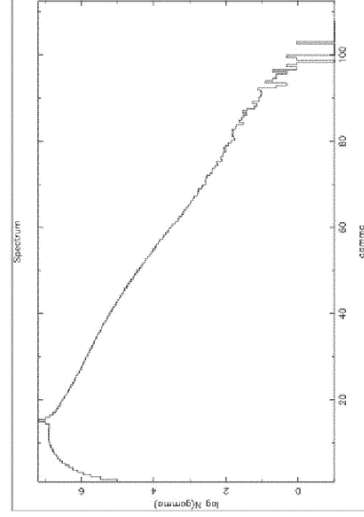
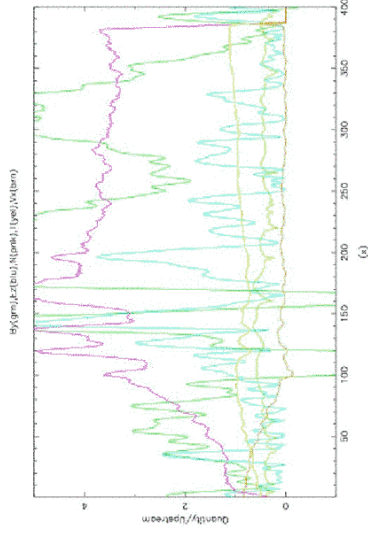
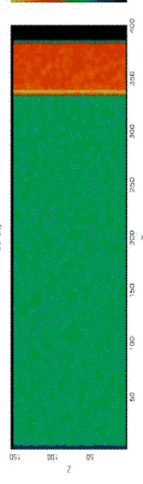
Shock structure  $\sigma=0.003$ : Mean B unimportant



Plane of  $v_x-B_y$



Plane of  $v_z-E_x$



### Perpendicular pair shocks: conclusions

Shock structure is controlled by magnetization parameter

$$\sigma = \omega_c^2 / \omega_p^2 = B^2 / (4\pi n \gamma m c^2) = (cr_L / \omega_p)^2$$

$\sigma < 0.005$  pair shocks are effectively unmagnetized.

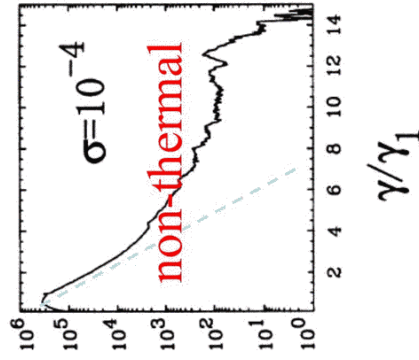
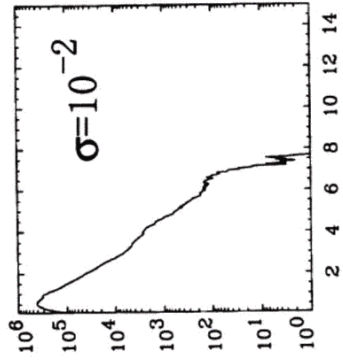
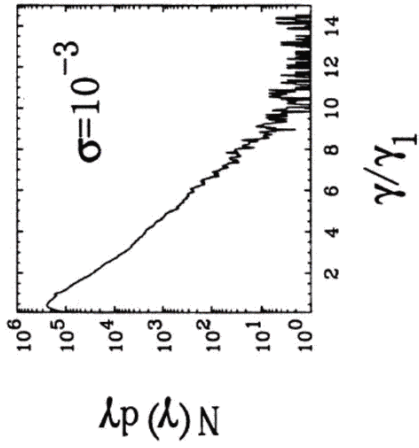
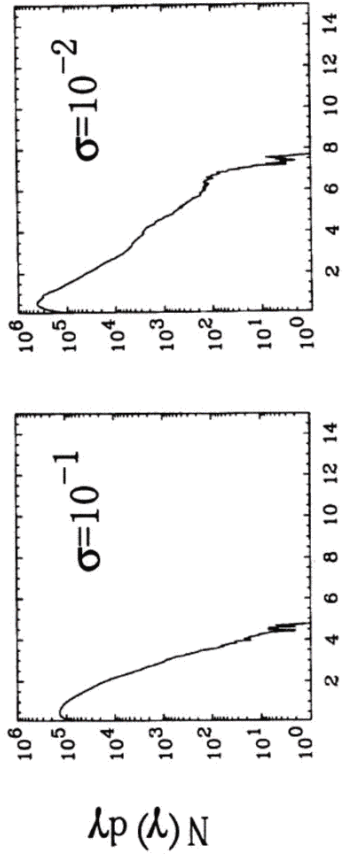
Such shocks don't have coherent magnetic overshoots characteristic of higher magnetization shocks.

Roughly, if the Larmor radius is larger than the Weibel shock lengthscale ( $r_L > 20c/\omega_p$ ,  $\sigma < 1/400 = 0.025$ ) Weibel instability dominates; for stronger B, cyclotron/synchrotron dynamics dominates - substantial coherence

Interestingly, even though in 1D coherent very low magnetization shocks are possible, in 3D they cannot exist -- Weibel instability dominates shock-drifting acceleration unlikely (Hoshino 2002)



**Perpendicular pair shocks: conclusions**

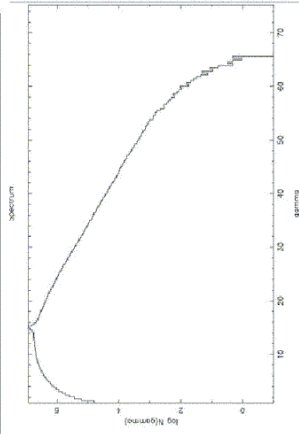
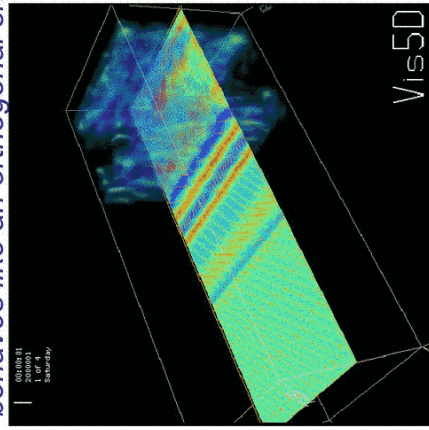


Hoshino 2002

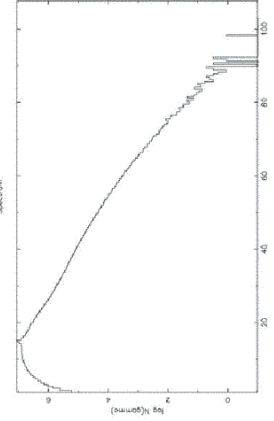
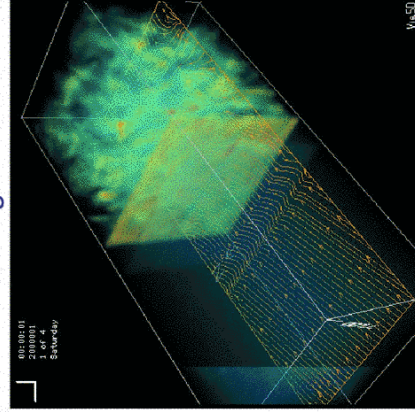
7

**Oblique pair shocks**

B field 45 degrees to the shock -- behaves like an orthogonal shock



B field 15 degrees to the shock normal -- behaves like unmagnetized shock



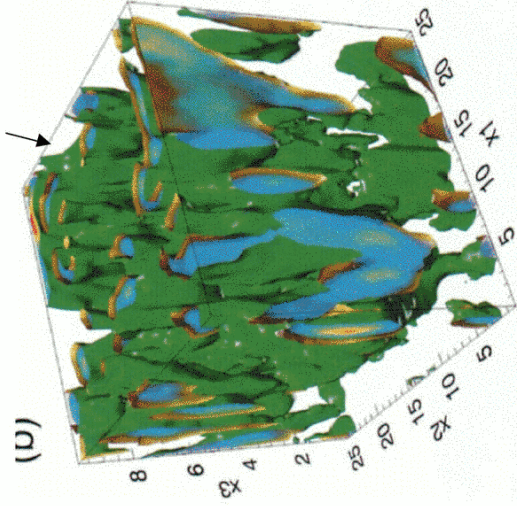
Shock structure parameterized by the transverse  $\sigma$

8

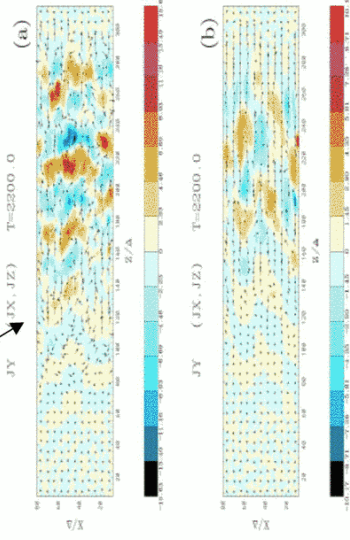
Magnetic reflection, cyclotron dynamics vs Weibel, diffusive dynamics:

$$\left(\frac{\delta B^2}{8\pi nT}\right)_{\sigma=0} \approx \left(\frac{\delta B^2}{8\pi\rho_1\gamma_1c^2}\right)_{\sigma=0} \approx 0.01 \text{ (magnetic trapping)} \Rightarrow \text{magnetic reflection dominates for } \sigma > 0.01 \text{ (observed)}$$

$\sigma=0$  results similar to Silva et al counterstreaming  $e^\pm$ , Nishikawa et al shocks



Magnetic filaments at  $41/\omega_p$ ;  
 Insufficient run time, reported nonthermal accel  $\rightarrow$  thermal dist after  $> 150/\omega_p$



Current filaments in plane  
 perp to filaments at  $27/\omega_p$ ;  
 run time insufficient, claimed  
 nonthermal dist = incomplete  
 thermalization <sup>9</sup>

Relativistic Shocks in Pairs: No evidence for non-thermal heating, all  $\sigma < 1$ .

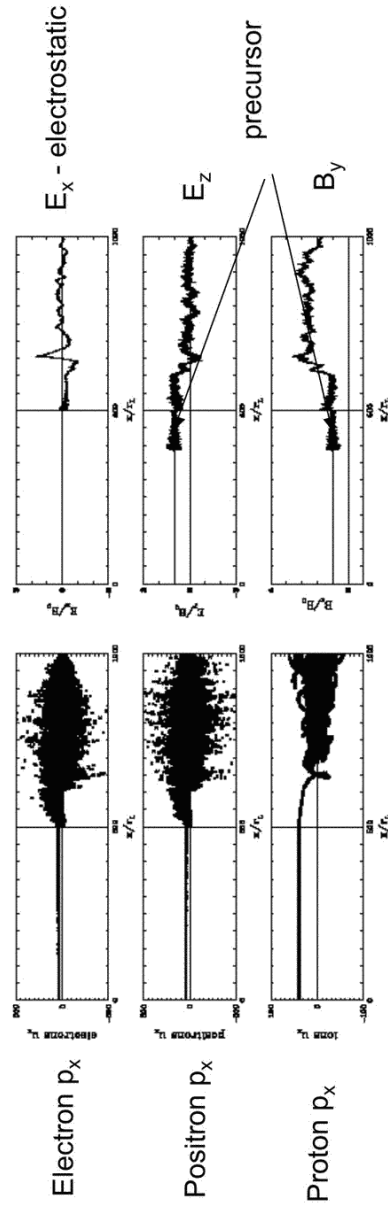
generation of permanent small scale B in Weibel shocks - evidence from simulations incomplete, but permanent magnetic energy (if any)  $\ll 1\%$  of upstream flow energy

Magnetized pair shocks have substantial coherence, possible coherent emission

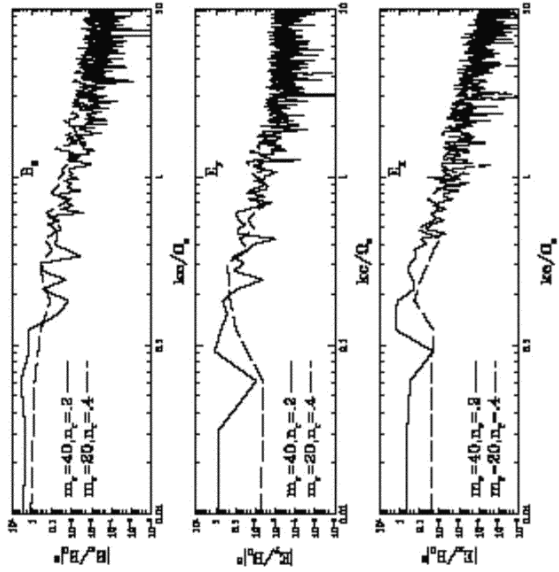
- relativistic shock EMP?

**Heavy Ion dynamics does show some nonthermal activity in 1D magnetic reflection models**

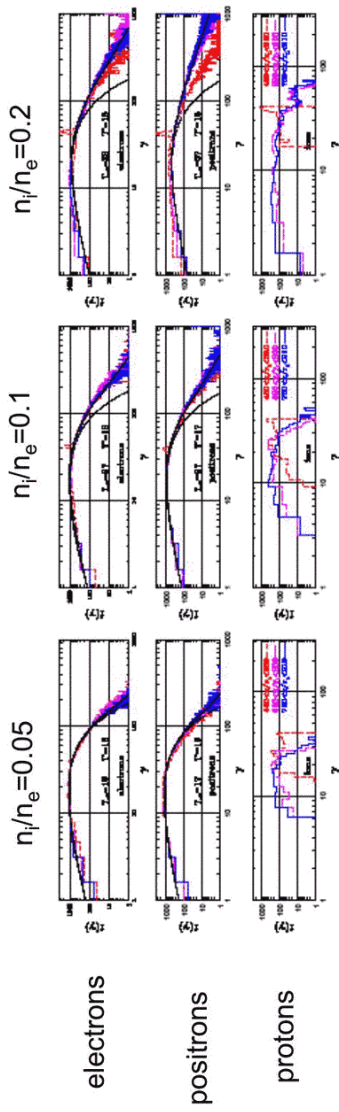
Same setup as for pure pair shocks in 1D, but now with protons (mass ratio 100)  
 $\sigma_1=0.03$



Acceleration due to cyclotron absorption of high harmonic ion cyclotron waves



11



$$N(\gamma) = f \frac{N_1}{T^\nu(T^\nu + 1)} \gamma \exp\left(-\frac{\gamma-1}{T^\nu}\right) + N_t \left(\frac{\gamma}{\gamma_m}\right)^{-\alpha} \left[1 - \exp\left(-\frac{\gamma-1}{\gamma_m}\right)\right]$$

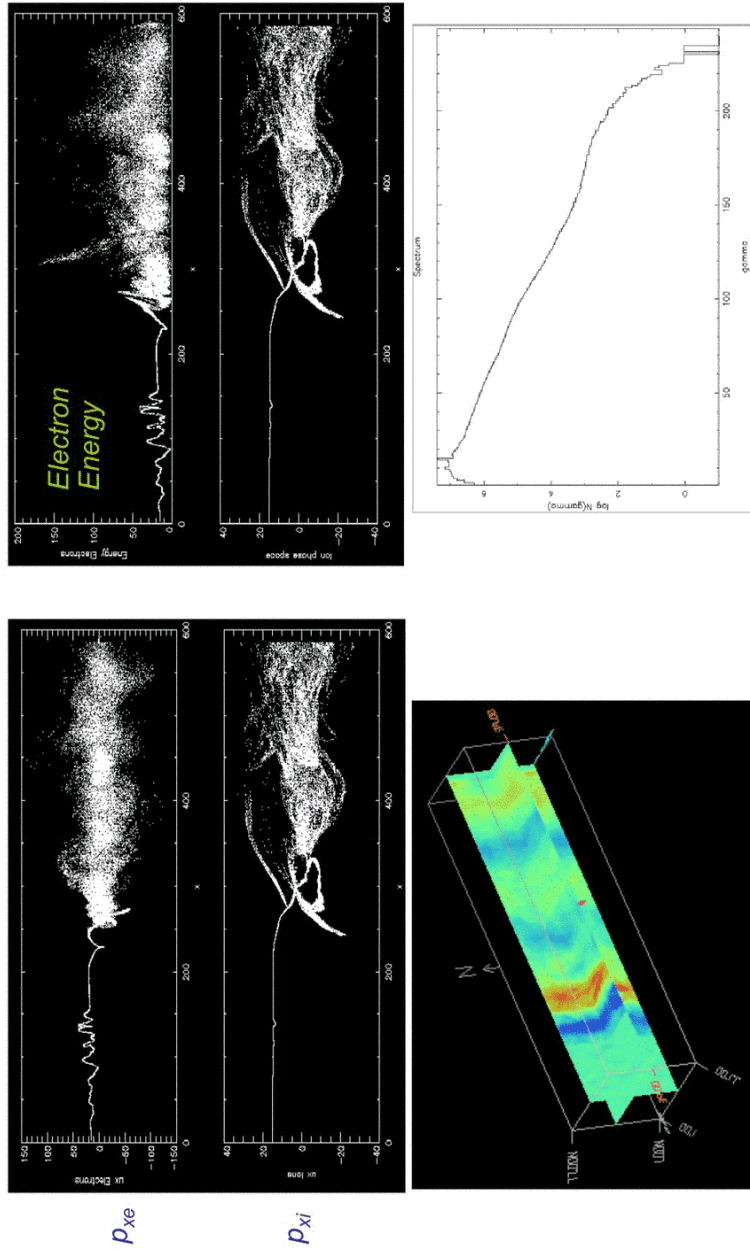
	$n_i/n_e = 0.05$		$n_i/n_e = 0.1$		$n_i/n_e = 0.2$	
	electrons	positrons	electrons	positrons	electrons	positrons
f	0.97	0.97	0.8	0.8	0.65	0.5
$T^\nu$	18	16	18	17	18	18
$\gamma_m$	100	100	100	90	100	85
$N_t$	20	20	130	120	160	190
$\alpha$	-3.5	-3.5	-3.2	-2.9	-2.6	-1.6
r	4	4	3	3	3	3
eff [%]	3	3	20	20	35	50

12

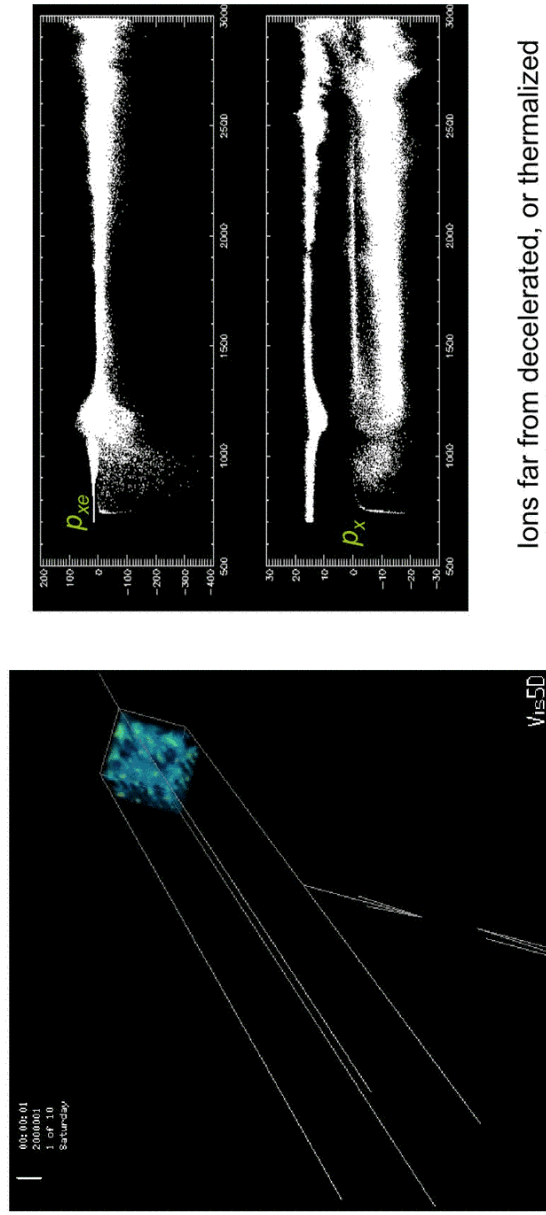


### Electron-ion shocks (3D)

Magnetization is mainly determined by ion energy density  $\sigma = B^2 / (4\pi n \gamma (m_i + m_e) c^2)$   
 Electrons are more magnetized than ions.  $\sigma = 0.1, m_i/m_e = 16$



### Unmagnetized ion-electron shock: $\sigma = 0, m_i/m_e = 16$

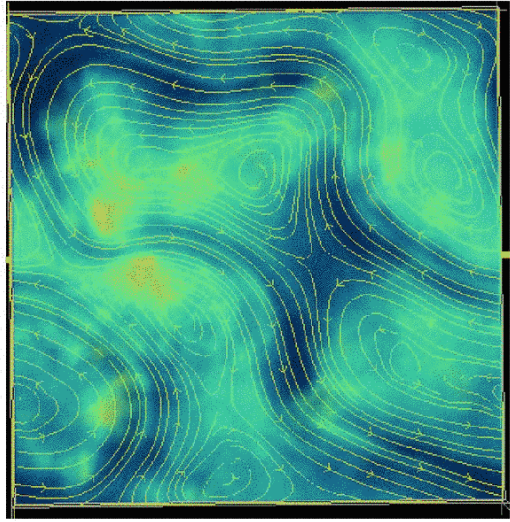


Ions far from decelerated, or thermalized  
 ( $t = 150(\omega_{pi})$ )

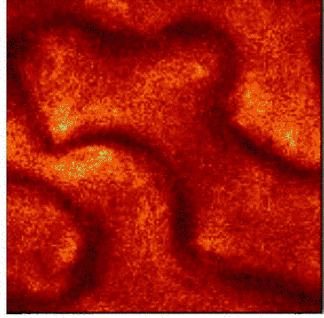
Electron Heating ("Acceleration") is by non-Fermi process, in the ion current channels (as in Hededal et al 04)

**Unmagnetized Electron-ion shocks: shielding**

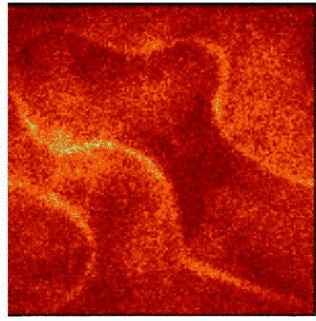
Unmagnetized ion-electron shock:  $\sigma=0$ ,  $m_i/m_e=16$



Ion density



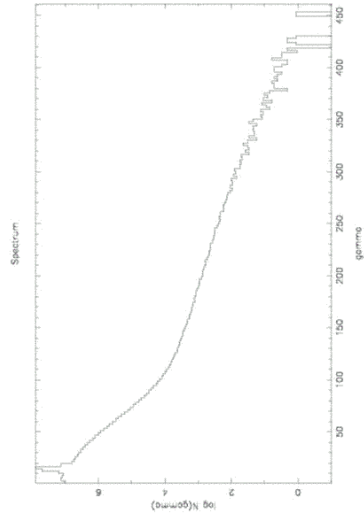
Electron density



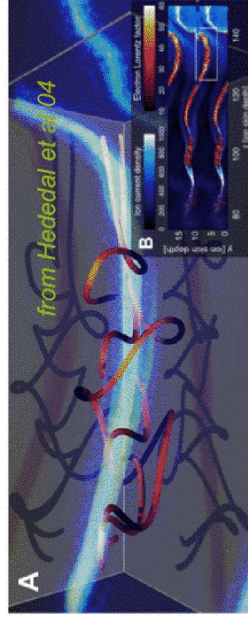
Electrons shield ion current filaments, slowing down the recombination of filaments.

15

Unmagnetized ion-electron shock:  $\sigma=0$ ,  $m_i/m_e=16$



Ion channel acceleration = 2nd order Fermi?  
Hot electron tail = hot Maxwellian? Nonthermal?



16

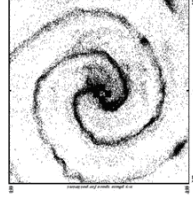
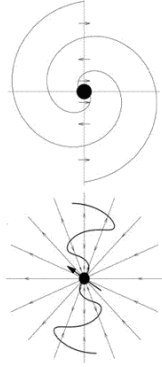
**Shock Conclusions**

Relativistic electron-positron shocks exist but are not **strong** nonthermal accelerators (efficiency < 1%). At low  $\sigma$ , they may generate small scale persistent B, but very small. Quite interesting as emitters of collective radiation (precursor, possible masers) from the particle reflection front when  $\sigma > 0.01$ . What happens at  $\sigma > 1$ ? - very coherent emitter?

Relativistic electron-positron, electron-proton shocks do show nonthermal acceleration due to resonant absorption of high harmonic ion cyclotron waves in 1D magnetic reflection shocks, but effect strong only when positrons are a minority - electron-ion shocks unclear, 3D "acceleration" in unmagnetized shocks comes from undecelerated ion beams in shock front leading edge; magnetized shocks in 3D shows vestiges of accel shown in 1D models, but effect weak (wrong polarization?) Shocks are Weibel dominated when  $B_0=0$  ( $\sigma < 0.01$ ), magnetic reflection dominated at higher  $\sigma$

$\sigma > 0.01$  electron-positron shocks may have more acceleration due to magnetic pumping (low frequency ion waves, pitch angle scattering by Weibel)

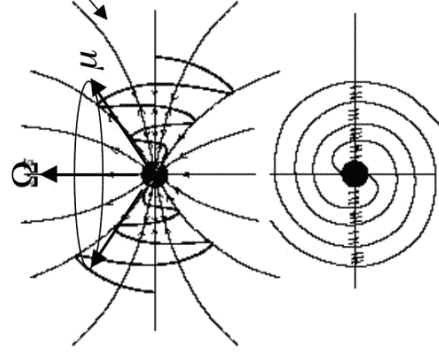
Non Shock acceleration for UHE - Surfing in Strong Waves



17

**WIND + WAVES (Michel, Usov, Coroniti, Melatos & Melrose, Lyubarsky, Kirk, JA)**

Analytic oblique split monopole (Bogovalov)



Current Sheets in equator require (proper) current  $J'$  perpendicular to equatorial plane

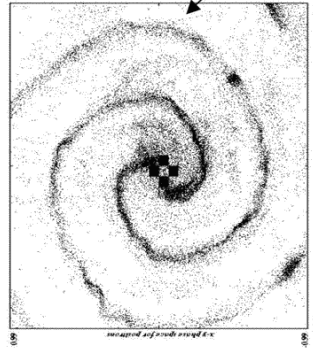
For "standard" pulsar parameters,

$$\frac{J'}{n'ec} > 1 \text{ for } r > 10^4 \lambda = R_{convert}$$

MHD of frozen in entropy wave "breaks"

Proposals:

- 1) "Reconnection", inductive heating dissipates wave component of very oblique rotator, leaves weak B of monopole like flow in asymptotic wind
- or
- 2) Entropy (slow?) mode converts to superluminal strong wave ( $a=e\delta E/mc\Omega \sim 10^7$ ), surf-riding acceleration



Active research area (by a very small group of people!)

2D PIC (NOT MHD) simulation of equatorial outflow, orthogonal rotator (Spitkovsky & Arons)

18



UHE Accelerator (?)

Linear (pondermotive surf-riding) acceleration in young rapidly rotating magnetar winds in normal galaxies (energetics similar to GRB)

